



FACULDADE DE
MEDICINA DENTÁRIA
UNIVERSIDADE DO PORTO

INTEGRATED MASTER IN DENTISTRY

SCIENTIFIC RESEARCH MONOGRAPH

**DEVELOPMENT OF DENTAL MSC-LOADED FIBRIN
HYDROGEL INJECTED INTO A 3D SCAFFOLD TO DRIVE
BONE TISSUE REGENERATION**

Patrícia Mafalda Gonçalves Alves

Porto, 2022

FACULTY OF DENTAL MEDICINE OF THE UNIVERSITY OF PORTO

INTEGRATED MASTER IN DENTISTRY

SCIENTIFIC RESEARCH MONOGRAPH

Scientific Area: Tissue Engineering, Regenerative Medicine and Stem Cells

**DEVELOPMENT OF DENTAL MSC-LOADED FIBRIN
HYDROGEL INJECTED INTO A 3D SCAFFOLD TO DRIVE BONE
TISSUE REGENERATION**

AUTHOR:

Patrícia Mafalda Gonçalves Alves ^{1,2,3}

Contact: up201803494@fmd.up.pt

SUPERVISOR:

Christiane Laranjo Salgado ^{2,3}

Contact: csalgado@ineb.up.pt

CO-SUPERVISOR:

Germano Neves Pinto da Rocha ¹

Contact: grocha@fmd.up.pt

¹FMDUP- Faculty of Dental Medicine of
the University of Porto, Porto, Portugal

²i3S- Institute for Research and
Innovation in Health of the University
of Porto, Porto, Portugal

³INEB- Institute for Biomedical
Engineering of the University of Porto,
Porto, Portugal

Acknowledgments

This master's dissertation is the result of a long journey composed of numerous obstacles, difficulties and uncertainties but also made of many challenges, discoveries and joys. Many times, choosing the best solution and direction along the way was only possible with the support, energy and strength of many people, to whom I am especially grateful and dedicate this moment of my life.

To my supervisor, Doctor Christiane Salgado, I express my deep gratitude, for her valuable and constructive suggestions during the development of the research work. I thank her for the genuine commitment, leadership and skilled guidance during this last phase of my university life and for having always steered me in the correct direction, contributing to further enhance my scientific knowledge and skills and awaken in me a desire and passion to continue to find innovative solutions in the area of dentistry.

To Professor Doctor Germano Rocha, I express my great appreciation, for having accepted to be my co-supervisor, and for his willingness to help and his enthusiastic encouragement.

To the Faculty of Dental Medicine of the University of Porto and all the professors of this institution, I thank for the outstanding dedication to teaching in this field of study and the vast knowledge shared during these years of continuous learning and professional and personal growth.

To the Institute for Research and Innovation in Health of the University of Porto, I am grateful for having welcomed and given me the opportunity to experience the area of research, for which I have developed a deep and special interest.

To my friends and classmates, I wish to thank for all the unforgettable moments we spent together, making my faculty life memorable.

Last but most certainly not least, I want to express my heartfelt gratitude to my parents, brother and grandparents for their unconditional support, encouragement and affection throughout my master's course. For believing in me and providing me with all the means to an excellent education, always with my well-being and best future in mind.

“The best way to predict the future is to create it.”

-Peter Drucker

Abstract

Introduction: Major oral bone defects are associated to trauma, osteonecrosis, tumor removal or congenital disorders. Over the past decades, bone tissue engineering (BTE) has arisen as a powerful tool for developing new bone treatment options to overcome shortages of existing bone graft materials and bone disease therapies. To address this challenge, BTE strategies have been directed to produce bone constructs that mimic natural bone structure regarding mechanical strength and microstructure. Collagen/nanohydroxyapatite (Coll/nanoHA) scaffolds and fibrin (Fb) hydrogels are examples of biomaterials widely used in the tissue engineering field.

Objectives: The authors intend to offer a three-dimensional (3D) Coll/nanoHA scaffold containing Human Dental Follicle Mesenchymal Stem Cells (hDFMSCs) into a fibrin/osteopontin (OPN) hydrogel in order to fully regenerate bone tissue and improve early recovery of patients with critical oral maxillofacial bone defects.

Methodology: Human osteoblast-like cell line (MG63) obtained from human osteosarcoma was first used as a pilot study to validate the protocol of cell delivery since it is a more reproducible cell line. Coll/nanoHA scaffolds (50:50 mass percentage) were produced by cryogelation technique, crosslinked, and full filled with a fibrin hydrogel with and without OPN loaded with MG63 or hDFMSCs cells. Cells proliferation, ECM production, osteogenic differentiation and cellular morphology were assessed through DNA content measure, total protein quantification, alkaline phosphatase (ALP) activity and confocal laser scanning microscopy (CLSM), respectively.

Results: Biologically, the composite collagen-nanohydroxyapatite/fibrin-osteopontin (Coll/nanoHA_Fb-OPN) exhibited high cellular proliferation, increasing the number of cells with time culture (7, 14 and 21 days). At day 21 of culture, hDFMSCs showed high ALP activity within Coll/nanoHA_Fb-OPN when compared to control group (Coll/nanoHA), indicating an early osteogenic differentiation. Also, CLSM images of the same Coll/nanoHA_Fb-OPN showed high OPN deposition by the hDFMSCs, corroborating with the ALP results. Thus, the presence of human OPN allowed the enhancement of those cells adhesion, migration, and spatial distribution within the 3D matrix and provided high cellular differentiation and proliferation.

Conclusions: This biomimetic Coll/nanoHA_Fb-OPN scaffold containing hDFMSCs may possess high osteoconduction, osteoinduction and osteogenesis properties and will favor new bone tissue formation and osteointegration. Hence, this innovative 3D biomaterial opened up a new prospect for the research of bone defect repair materials in BTE as it has been evidenced to be a potential solution that shall further improve effective bone tissue regeneration.

Key-words: Biomaterials; Hydrogel; Fibrin; Collagen; Nanohydroxyapatite; Osteopontin, Oral maxillofacial bone tissue regeneration

Resumo

Introdução: Os principais defeitos ósseos orais estão associados a traumas, osteonecrose, remoção de tumores ou doenças congênitas. Nas últimas décadas, a engenharia de tecido ósseo (BTE) surgiu como uma ferramenta para o desenvolvimento de novas opções de enxerto ósseo de modo a superar as limitações dos materiais de regeneração óssea existentes e terapias de doenças ósseas. Para responder a este desafio, as estratégias BTE têm sido conduzidas para produzir scaffolds que mimetizam a estrutura óssea natural em relação à resistência mecânica e à microestrutura. Os scaffolds de colagénio/nanohidroxiapatite (Collagen/nanoHA) e o hidrogel de fibrina (Fb) são exemplos de biomateriais amplamente utilizados no campo da engenharia de tecidos.

Objetivos: Os autores tem como objetivo final, produzir um scaffold tridimensional (3D) à base de Coll/nanoHA contendo células mesenquimais do folículo dentário humano (hDFMSCs) presentes dentro de um hidrogel à base de fibrina e osteopontina (OPN) para regenerar completamente o tecido ósseo e reduzir o período de recuperação de pacientes com defeitos ósseos oro-maxilo-faciais críticos.

Metodologia: Pré-osteoblastos humanos (MG63) isolados a partir do osteossarcoma humano foram primeiramente utilizados em um estudo piloto com o objetivo de validar a viabilidade destas células quando introduzidas no hidrogel e injetadas no interior do scaffold, uma vez que se trata de uma linha celular mais reprodutível. Os scaffolds Coll/nanoHA (percentagem de massa 50:50) foram produzidos pela técnica de criogelação, reticulados, e preenchidos com um hidrogel de fibrina contendo ou não OPN e células (MG63 ou hDFMSCs). A proliferação celular, produção de matriz extracelular, diferenciação osteogénica e morfologia das células foram avaliadas através da quantificação do ADN, da proteína total, da atividade de fosfatase alcalina (ALP) e por imagens de microscopia confocal de varredura a laser (CLSM), respectivamente.

Resultados: Biologicamente, o composto colagénio-nanohidroxiapatite/fibrina-osteopontina (Coll/nanoHA_Fb-OPN) demonstrou uma elevada proliferação celular, aumentando o número de células ao longo do tempo de cultura (7, 14 e 21 dias). No 21º dia de cultura, hDFMSCs apresentaram uma elevada atividade da enzima ALP dentro do scaffold de Coll/nanoHA_Fb-OPN quando comparado com o grupo controlo (Coll/nanoHA), indicando uma diferenciação osteogénica precoce. Além disso, imagens de CLSM do mesmo scaffold de Coll/nanoHA_Fb-OPN mostraram uma elevada deposição de OPN pelas hDFMSCs, corroborando os resultados da atividade da ALP. Portanto, a presença de OPN humana permitiu uma melhoria da adesão, migração e distribuição espacial dessas células dentro da matriz 3D e proporcionou uma elevada diferenciação e proliferação celular.

Conclusões: O scaffold biomimético Coll/nanoHA_Fb-OPN contendo hDFMSCs possui elevadas propriedades de osteocondução, osteoindução e osteogénese e poderá favorecer a sua osteointegração e formação de novo tecido ósseo. Em conclusão, este inovador

biomaterial 3D fomentará uma nova perspectiva para o desenvolvimento de materiais para BTE e a completa reparação de defeitos ósseos críticos, uma vez que comprovou ser uma solução adequada que irá garantir a regeneração efetiva do tecido ósseo.

Palavras-chave: Biomateriais; Hidrogel; Fibrina; Colagénio; Nanohidroxiapatite; Osteopontina; Regeneração do tecido ósseo oro-maxilo-facial

Contents

Acknowledgments	III
Abstract	VII
Resumo	IX
List of Figures	XIII
List of Abbreviations	XV
Chapter 1- Objectives and Document Structure	3
1.1 Objectives of the work	3
1.2 Document structure.....	3
Chapter 2- Literature Review	7
2.1 Introduction.....	7
2.2 Bone.....	8
2.2.1 Function	8
2.2.2 Formation.....	8
2.2.2.1 Intramembranous Ossification.....	8
2.2.3 Structure	9
2.2.4 Constitution	10
2.2.4.1 Collagen.....	12
2.2.4.2 Hydroxyapatite	13
2.2.5 Bone Repair Process	13
2.2.5.1 Osteopontin in Bone Repair	14
2.3 Bone Tissue Engineering.....	15
2.3.1 Scaffolds	15
2.3.2 Biomaterials.....	16
2.3.2.1 Polymer/Bioceramic Scaffolds.....	17
2.3.3 Hydrogels in Bone Tissue Engineering.....	18
2.3.3.1 Classification of Hydrogels	19
2.3.3.2 Fibrin-based Hydrogel	20
2.3.3.3 Fibrin-based Hydrogel in Bone Tissue Engineering	20
2.3.4 Cells.....	21
2.3.4.1 Human Dental follicle Stem Cells (hDFSCs)	21
Chapter 3- Materials and Methods	25

3.1 Materials	25
3.2 Fibrin Hydrogel (with and without OPN)	25
3.2.1 Preparation of Fibrin Hydrogel	25
3.2.2 Preparation of OPN	25
3.2.3 Preparation of Fibrin - OPN Hydrogel	26
3.3 <i>In vitro</i> biological studies	26
3.3.1 Establishment of Stem Cell Cultures from the Human Dental Follicle (hDFMSC)	26
3.3.2 Cell Culture	26
3.3.3 Cellular Proliferation Assay	26
3.3.4 Cellular Differentiation Assay and Protein Quantification	27
3.3.5 Confocal Laser Scanning Microscopy (CLSM)	27
3.3.6 Statistical Analysis	28
3.4 Preparation of Collagen/nanohydroxyapatite Scaffolds	28
3.5 Preparation of Coll/nanoHA - Fibrin Hydrogel composite	28
Chapter 4- Results	33
4.1- <i>In vitro</i> Biological Studies: MG63	33
4.1.1- DNA Quantification Assay	33
4.1.2- Total Protein Content	33
4.1.3- Alkaline Phosphatase (ALP) Activity	34
4.1.4- Confocal Laser Scanning Microscopy	35
4.2- <i>In vitro</i> Biological Studies: hDFMSCs	38
4.2.1- DNA Quantification Assay	38
4.2.2- Total Protein Content	39
4.2.3- Alkaline Phosphatase (ALP) Activity	39
4.2.4- Confocal Laser Scanning Microscopy	40
Chapter 5- Discussion	45
Chapter 6- Conclusion and Future Outlook	51
References	53
Appendix A	61
Appendix B	62

List of Figures

Figure 1- Diagrams of intramembranous ossification.....	9
Figure 2- Hierarchical architecture of bone tissue from macroscopic to nanometer level ...	10
Figure 3- Bone tissue cells: bone-lining, osteoblasts, osteocytes and osteoclasts	11
Figure 4- Collagen type I: hierarchical levels of the fibril organization	12
Figure 5- Stages of bone fracture healing mechanism	14
Figure 6- Classification of biodegradable polymers commonly used in biomedical applications based on their source (natural, synthetic, or semi-synthetic).....	17
Figure 7- Hydrogel chemical structure representation	19
Figure 8- Total DNA content of MG63 cells within Coll/nanoHA_Fb, Coll/nanoHA_Fb-OPN, and Coll/nanoHA biocomposite scaffolds after 3, 7 and 14 days of culture in basic medium. Statistical differences between samples from different time-points, *p <0.05 and **p <0.01	33
Figure 9- The total protein concentration for MG63 cells (ECM) within Coll/nanoHA_Fb, Coll/nanoHA_Fb-OPN, and Coll/nanoHA biocomposite scaffolds after 3, 7 and 14 days of basic culture. Statistical differences between samples from different time-points, *p <0.05 and ****p <0.0001	34
Figure 10- ALP activity of MG63 osteoblast-like cells culture within Coll/nanoHA_Fb, Coll/nanoHA_Fb-OPN, and Coll/nanoHA biocomposite scaffolds after 3, 7 and 14 days of culture. Statistical differences (p >0,05) were not observed	35
Figure 11- Confocal laser scanning microscopy (CLSM) images showed the human ECM (osteopontin) of MG63 after 3, 7 and 14 days of culture within Coll/nanoHA_Fb scaffold (with and without OPN). MG63 nuclei were stain in blue and human OPN in green. Scale bar: 100 µm	36
Figure 12- CLSM image of MG63 osteoblast-like cells cultured within Coll/nanoHA (50:50) biocomposite scaffolds after 21 days of culture (normal morphology)	37
Figure 13- Confocal laser scanning microscopy (CLSM) images showed the morphology of MG63 after 3, 7 and 14 days of culture within a Coll/nanoHA_Fb scaffold (with and without OPN). MG63 nuclei were stain in blue and cytoplasm (actin filaments) in red. Scale bar: 100 µm	37

Figure 14- Total DNA content expression of hDFMSCs proliferation rate in Coll/nanoHA_Fb, Coll/nanoHA_Fb-OPN, and Coll/nanoHA biocomposite scaffolds for 7, 14 and 21 days of culture in basic medium. Statistical differences between samples from different time-points, *p <0.05, **p <0.01 and ***p <0.001	38
Figure 15- The total protein secreted by hDFMSCs (ECM) in Coll/nanoHA_Fb, Coll/nanoHA_Fb-OPN, and Coll/nanoHA biocomposite scaffolds after 7, 14 and 21 days of culture. Statistical differences between samples from different time-points, *p <0.05, *** p <0.001 and ****p <0.0001	39
Figure 16- ALP activity of hDFMSCs culture within Coll/nanoHA_Fb, Coll/nanoHA_Fb-OPN, and Coll/nanoHA biocomposite scaffolds after 7, 14 and 21 days. Statistical differences between samples from different time-points, *p <0.05, *** p <0.001 and ****p <0.0001	40
Figure 17- CLSM images showed the human osteogenic ECM (OPN) regarding hDFMSCs after 7, 14 and 21 days of culture within Coll/nanoHA_Fb scaffold (with and without OPN) and Coll/nanoHA scaffold. hDFMSCs nuclei were stain in blue and human OPN in green. Scale bar: 100 µm	41
Figure 18- CLSM images showed the morphology of hDFMSCs after 7, 14 and 21 days of culture within a Coll/nanoHA_Fb scaffold (with and without OPN) and Coll/nanoHA scaffold. hDFMSCs nuclei were stain in blue and cytoplasm (actin filaments) in red. Scale bar: 100 µm	42
Figure 19- Total DNA content of MG63 osteoblast-like cells within Coll/nanoHA and Coll/nanoHA_Fb biocomposite scaffolds for 1, 3 and 7 days of culture in basic medium. Statistical differences between samples from different time-points (****p <0.0001)	61
Figure 20- ALP activity of MG63 osteoblast-like cells culture in Coll/nanoHA and Coll/nanoHA_Fb biocomposite scaffolds after 1, 3 and 7 days of culture. Statistical differences (p >0,05) were not observed	61
Figure 21- Total DNA content of MG63 osteoblast-like cells within Coll/nanoHA and Coll/nanoHA_Fb biocomposite scaffolds for 3, 7 and 14 days of culture in basic and osteoinductive medium. Statistical differences between samples from different time-points, **p <0.01, ***p <0.001 and ****p <0.0001	62

List of Abbreviations

3D	three-dimensional
%	percentage
°C	degree celsius
ALP	alkaline phosphatase
BGs	bioactive glasses
BMPs	bone morphogenetic proteins
β-TCP	beta-tricalcium phosphate
BTE	bone tissue engineering
CaCl ₂	calcium chloride
CLSM	confocal laser scanning microscopy
Cm ²	square centimeter
Coll	collagen
CO ₂	carbon dioxide
DAPI	4'-6-diamidine-2-phenylindole
DFSCs	dental follicle stem cells
DMEM	dulbecco's modified eagle medium
DNA	deoxyribonucleic acid
ECM	extracellular matrix
EDC	1-ethyl-3-(3-dimethyl aminopropyl) carbodiimide hydrochloride
EDTA	ethylenediaminetetraacetic acid
Fb	fibrin
FBS	fetal bovine serum
HA	hydroxyapatite
HCl	hydrochloric acid
hDFMSCs	human dental follicle mesenchymal stem cells

KCl	potassium chloride
mg	milligram
MG63	human osteoblast-like cell
min	minute
mL	milliliter
MSC	mesenchymal stem cell
μg	microgram
μL	microliter
μm	micrometer
NaCl	sodium chloride
nanoHA	nanohydroxyapatite
NaOH	sodium hydroxide
NHS	n-hydroxysuccinimide
NIH	national institute of health
nm	nanometer
OPN	osteopontin
PBS	phosphate buffered saline
PFA	paraformaldehyde
pH	potential of hydrogen
SCs	stem cells
Tb	thrombin
TBS	tris-phosphate buffered saline
TCP	tricalcium phosphate
TRIS	hydroxymethyl aminomethane

CHAPTER 1

Objectives and Document Structure

Chapter 1- Objectives and Document Structure

1.1 Objectives of the work

Nowadays, the challenges related to maxillofacial bone regeneration are the difficulties in achieving extracellular biomimetic requirements (inorganic and organic matrix) and inability to produce complex, but more functional cellularized structures in large 3D scaffolds. To develop solutions for these clinical issues, the main goal of this master thesis work is to offer a 3D collagen-nanohydroxyapatite scaffold containing human MSC-loaded fibrin/osteoontin hydrogel in order to fully regenerate bone tissue and improve early recovery of patients with critical maxillofacial bone defects. This biomimetic scaffold will generate the necessary three-dimensional microenvironment to host cells and allow proliferation, differentiation and production of mineralized extracellular matrix leading to a final self-organized bone structure.

The fibrin hydrogel (with or without Osteopontin - OPN) and the composite 3D biomaterial (Coll/nanoHA + fibrin/OPN gel) were loaded with human pre-osteoblast cells (MG63) or primary human follicle MSCs (hDFMSCs) to test *in vitro* efficiency and safety, the main objectives are:

- To evaluate the cellular behaviour within the modified hydrogel, direct contact assay was performed according to ISO 10993-5:2009 with standard cell line (MG63) or human dental follicle MSCs (hDFMSCs) that were loaded into the fibrin gel (with OPN or not) and after that, injected into the scaffold.
- The cellular profile includes the evaluation of the cell morphology, proliferation rate and osteogenic differentiation (Alkaline Phosphatase activity).

1.2 Document structure

This master thesis is organized into chapters. Chapter 2 addresses the literature review, and the state of the art. Chapter 3 approaches the methodology applied in this work, describing the biological characterization of the materials in the study. Chapter 4 presents the results obtained, and in chapter 5 their suitable discussion. Finally, chapter 6 presents the conclusions and future perspectives of the work developed.

CHAPTER 2

Literature Review

Chapter 2- Literature Review

2.1 Introduction

Over the past decades, bone tissue engineering (BTE) has emerged as a powerful tool for developing new bone treatment options to overcome shortages of existing bone graft materials and bone disease therapies. In recent years, BTE strategies have been centered on producing bone constructs that mimic natural bone structure regarding mechanical strength and microstructure [1,2]. In this context, the production of accurate biomaterials for BTE should be broadly based on several components: (1) a biocompatible scaffold that resembles extracellular matrix (ECM), (2) osteogenic cells to build the bone tissue matrix, (3) biological clues such as growth factors to guide mesenchymal cells towards bone phenotype, and (4) material/host interactions mediated by immune cells that favor the bone healing [1,3,4].

Major bone defects are linked to trauma, osteonecrosis, tumor removal or congenital disorders. The use of bone autografts continues to be the *gold standard* surgical treatment for reconstructing bone defects, despite being associated to higher morbidity. This is closely linked to the need for obtaining considerable amounts of bone from donor-site and as a consequence the donor area is left for self-healing. However, commercially available products are unable to reproduce the complex bone structure, resulting in undesirable effects such as foreign body response, lack of regenerative capacity, high degradation rate, and failure in long-term applications [5].

Synthetic bone scaffolds seeded with multipotent stem cells are used with success in tissue engineering for bone regeneration. The stem cells (SCs) are progenitors' cells with clonogenicity, multi-lineage differentiation and self-renewal capability. In the literature, SCs can be originated by various oral donor tissues, for example deciduous elements, the periodontal ligament, the dental follicle, dental pulp, apical papilla and gingival tissue [6].

Moreover, MSCs together with biomaterials, as a bone graft, possess a major regenerative capability as a tissue engineered device and should be able to deliver higher regenerative and remodeling capacity of the bone tissues through osteoconduction, osteoinduction and osteogenesis properties with high levels of newly formed bone and osteointegration [6].

2.2 Bone

2.2.1 Function

Bone is structurally and functionally a highly dynamic and diverse tissue that possesses the ability to achieve a full range of functions and is able to react to a large variety of metabolic, physical and endocrine stimuli. Bone is a complex living tissue responsible for (1) the mechanical support and our body locomotion, (2) the regulation of systemic acid-base balance, (3) the vital organ protection, (4) the production of biological elements required for hematopoiesis, (5) the maintenance of the homeostasis with the key electrolytes (via calcium and phosphate ion storage) and (6) the entrapment of dangerous metals (e.g., lead, nickel, chromium). In addition, bone is involved in a continuous cycle of resorption and renewal. It is subject to a steady chemical exchange and structural remodeling as a consequence not only of internal mediators, but also external mechanical demands [4,7-11].

2.2.2 Formation

Bone formation begins as early as the foetal stage and continues through adulthood [11,12]. As bone is a mineralized organ, ossification is one of the most critical processes in bone development, being controlled by two distinct mechanisms: intramembranous and endochondral ossification, which are determined by different differentiation pathways [11-17]. Osteochondral progenitors differentiate into osteoblasts to originate the new bone during intramembranous ossification. During endochondral ossification, osteochondral progenitors differentiate into chondrocytes instead and form a cartilage template of the future bone [4,11-13]. The ossification process is dependent on the type of bone being formed. Intramembranous ossification is involved in the formation of flat and irregular shaped bones, such as the craniofacial structures including skull, mandible and maxilla. Endochondral ossification is involved in the formation of long bones, such as the femur, tibia, humerus, metacarpal and vertebrae [4,8,11,15,16].

2.2.2.1 Intramembranous Ossification

Intramembranous ossification occurs due to the direct differentiation of MSCs into bone-forming osteoblasts, leading to newly formed osteoblasts that start to synthesize a collagenous bone matrix, which later becomes mineralized [11,15-18]. Intramembranous ossification starts from mesenchymal condensation and progresses through development of the ossification center, followed by ossification expansion, trabecula formation, compact bone formation and periosteum development (Fig. 1) [11,16,18]. The osteoblasts first

appear in the condensation secrete bone matrix that forms the ossification center. The early osteoblasts secrete osteoid, an uncalcified matrix, characterized by randomly oriented collagen fibrils, known as woven (primary) bone. This matrix calcifies soon after, while the osteoblasts mature and finally differentiate into osteocytes, becoming encapsulated and entrapped into the osteoid. As osteoblasts differentiate into osteocytes, more mesenchymal progenitor cells around the osteoid surface differentiate into new osteoblast cells to expand the calcification center. Osteoid expansion surrounding the capillaries results in a trabecular matrix of spongy bone, whereas osteoblasts on the superficial layer become the periosteum, a protective layer of compact bone. The blood vessels grow alongside with other cells, between the trabecular bone, and form the red marrow [8,16-18].

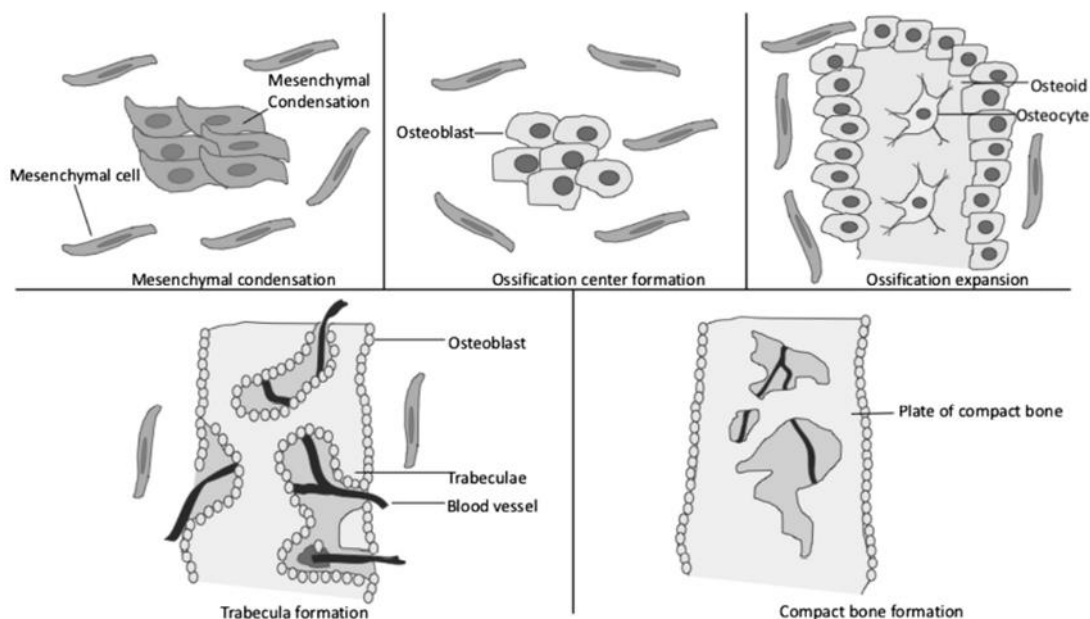


Figure 1- Diagrams of intramembranous ossification [16].

2.2.3 Structure

Natural bone is a physiologically mineralized type of connective tissue that achieves its multiple diverse functions and excellent mechanical properties due to its hierarchical manner organization, from the nano to the macro scale (Fig.2) [9,18]. At the bone macroscopy level, two types of architecture structures are distinguished, based on their structural, metabolic and mechanical function: cortical or compact bone and trabecular or cancellous bone, in a ratio of 80:20 of the percentage of total bone mass of an adult skeleton [8,11,19,20]. The first one is 80–90% mineralized, has lower blood vessel presence and constitute the outer part of the tissue; contrarily, cancellous bone is higher vascularized, shows a sponge-like structure with interconnecting cavities with approximately 75%-85% porosity and is located at the internal section of bone [8,9,18,20].

At the microscopic level, cortical bone is composed of multiple lamellae, about 3 μm thickness and ground substance, arranged in concentric layers, surrounding a vertical Haversian canal that is parallel to the long axis of the bone. Volkmann's canals are interconnected with the Haversian canals containing blood vessels, nerves, connective tissue and lymphatic vessels. Between each canal, there is a small-scale cavity known as lacunae which is interconnected with a series of tunnels called canaliculi. This hole structure is nominated osteon or Haversian system, and it is considered the functional unit of bone tissue [9,11,18,20]. Trabecular bone is composed of large spaces, with an interconnected network of parallel trabecular plates. The matrix consists in a 3D network of fine columns that interlink to each other forming the trabeculae. The spaces between trabeculae are filled with bone marrow, blood vessels and a fibrous connective tissue layer called periosteum that surrounds the external surface of cortical bone, while in the internal section, a membranous structure - the endosteum - covers the surface of the cortical and the trabecular bone [11,18-20].

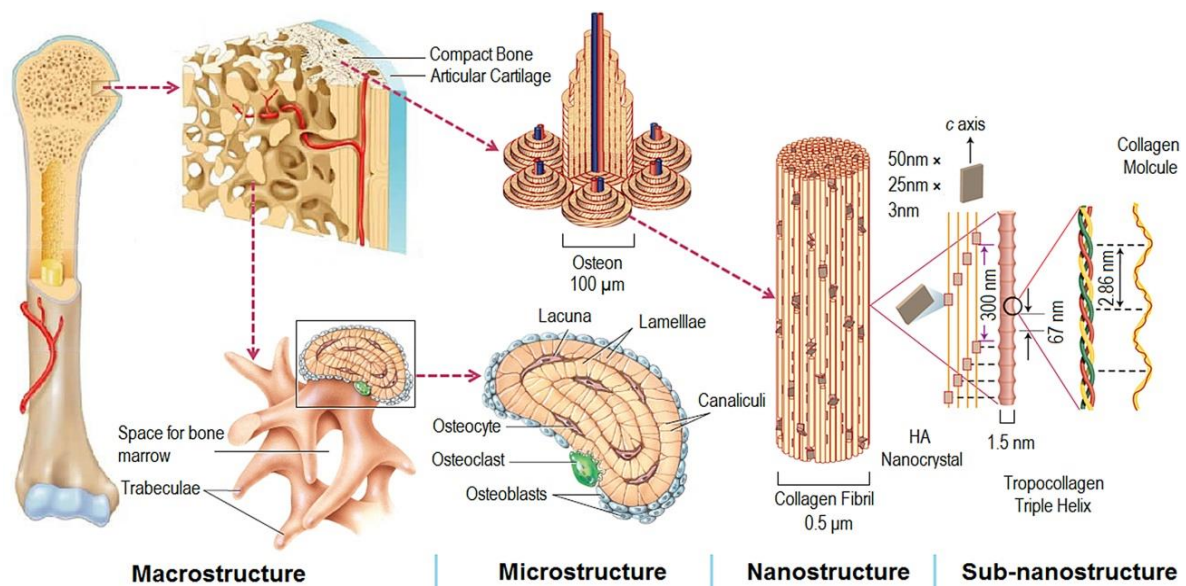


Figure 2- Hierarchical architecture of bone tissue from macroscopic to nanostructure level [21].

2.2.4 Constitution

Mammalian bone is composed by inorganic salts and organic matrix. The organic matrix corresponds to one third of bone in weight, mainly formed by proteins where collagen type I represents approximately 95% and the remaining 5% is composed of proteoglycans and numerous non-collagenous proteins [7,10,11,18,19,22,23]. The bone ECM has a 65% dry weight of mineral matrix, mainly formed of non-stoichiometric calcium phosphate and calcium carbonate in small crystals of hydroxyapatite with nanometric size. Binding with collagen, the non-collagenous matrix proteins serve as a scaffolding template

for hydroxyapatite deposition whose association is responsible for the typical stiffness and resistance of bone tissue [7,11,19,22,23]. Water is the third major component of the bone tissue that ranges from 5 to 10% of the total bone composition. It can be bound to the mineral-collagen composite, or it can flow freely through canalicular and vascular vessels in bone [11,18].

Besides mineralized bone milieu, the four most important cells present in bone matrix are: osteogenic or bone-lining cells, osteoblasts, osteocytes, and osteoclasts, whose structure is shown in Figure 3 [7,10,11,19,23]. Osteoblasts are fully differentiated cells that aim at the synthesis, deposition and mineralization of the bone matrix by producing a protein mixture called osteoid, controlling calcium and mineral deposition and also remodeling of bone. Osteocytes comprise 90–95% of the total bone cells extending filopodial processes through canaliculi to contact neighboring cells and blood vessels, overcoming the limited diffusion of nutrients and metabolites through the mineralized matrix. Furthermore, they have an active role in bone remodeling, through regulation of osteoblast and osteoclast activities. Osteoclasts are rich in mitochondrias and lysosomal vesicles that release enzymes and acids that foster bone resorption. Osteoclasts also help to remodel injured bones and create pathways for nerves and blood vessels to grow through. Lastly, bone-lining cells are able to regulate calcium hemostasis, osteoclastic differentiation and play a significant role in the bone remodeling process [7,10,11,19,23].

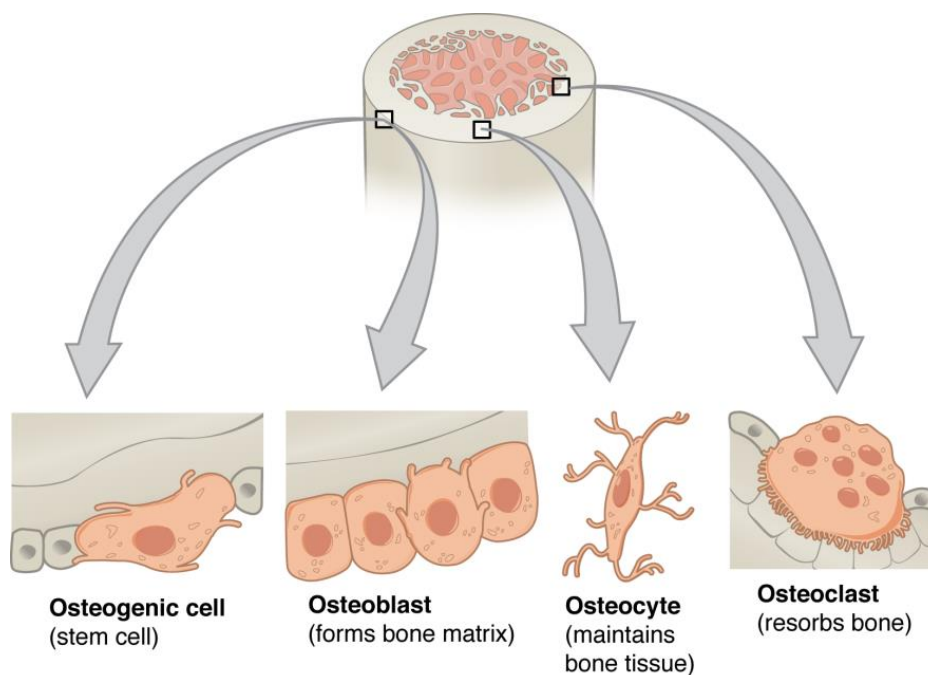


Figure 3- Bone tissue cells: bone-lining, osteoblasts, osteocytes and osteoclasts [7].

2.2.4.1 Collagen

Almost 80-90% of the total proteins present in the extracellular matrix of bone tissue are members of the collagen family, and Collagen type I comprises approximately 95% of the total collagen content [11,24-26]. Other types of collagen, such as types III and V, are present at low levels in bone and appear to modulate the Collagen type I fibril diameter [26]. Each molecule of Collagen type I possesses domains with repetitions of the proline-rich tripeptide Gly-X-Y and is typically composed of three intertwining polypeptide chains, two identical $\alpha_1(I)$ -chains and one $\alpha_2(I)$ -chain, with a helical twist around each other in a characteristic triple helix [11,24-26].

Collagen fibrils are composed of tropocollagen molecules with approximately 300 nm in length and 1.5 nm in diameter, with molecular axes parallel to fibril direction. This structure creates an observable interval of 67 nm length called the D-band. There is a space between two consecutive collagen molecules that measures 0.6 D or about 40 nm, where hydroxyapatite crystals grow and are responsible for the mineralization of these collagen fibrils (Fig. 4). After that, in a hierarchical level, the combination of multiple collagen fibrils forms the collagen fiber [24,26].

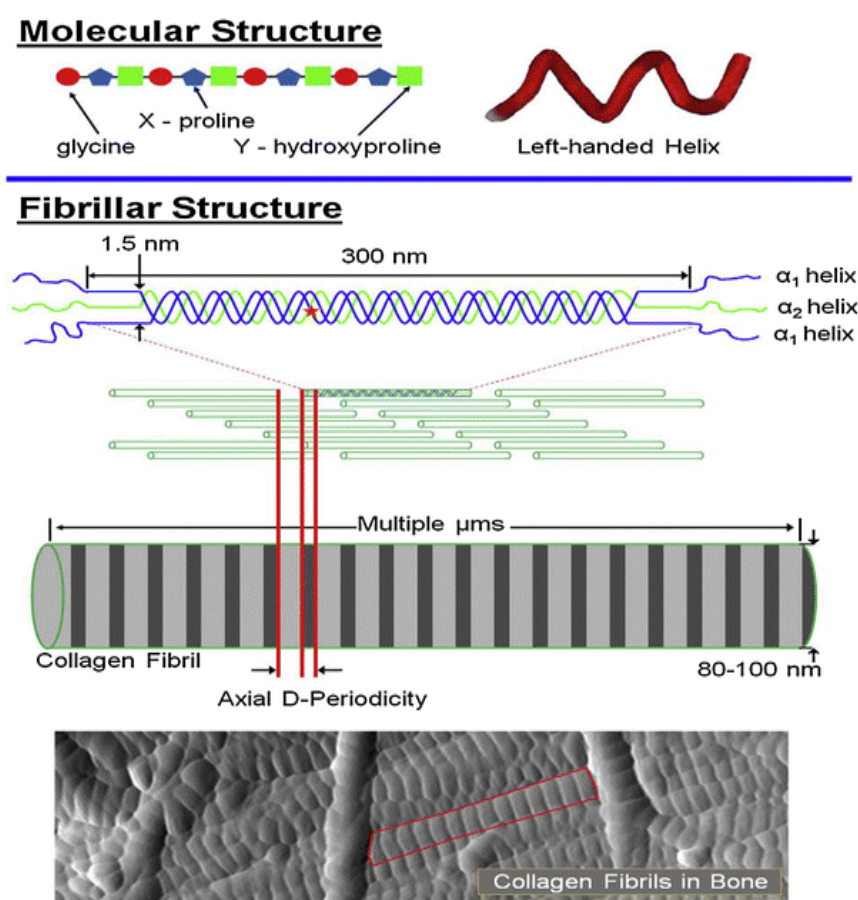


Figure 4- Collagen type I: hierarchical levels of the fibril organization [26].

2.2.4.2 Hydroxyapatite

Hydroxyapatite (HA), $(\text{Ca}_{10}(\text{PO})_6(\text{OH})_2)$ is considered the most important inorganic constituent of bone, containing about 70% in dry weight of bone tissue. It is observed as tiny nanocrystals of apatite platelets, often about 15–200 nm long, 10–80 nm wide and with thickness of 2-7 nm. The formation of HA particles is named as mineralization process where collagen fibrils act as a template for nucleation and modulation of HA particles favouring the crystals' growth within the collagen fibrils [11,12,28,29].

2.2.5 Bone Repair Process

Bone tissue, when injured, possess a unique ability to self-heal without the formation of scar tissue. Bone fracture regeneration occurs via a cascade of signaling molecules and involves the coordination of biological responses such as the progenitor cells recruitment along with inflammatory, endothelial and hematopoietic cells, followed by a sequence of events similar to intramembranous long bone formation. Fracture healing undergoes four histologically distinguishable stages as displayed at Figure 5, such as the hematoma formation, fibrocartilaginous callus formation, bony callus formation and bone remodeling.

At the fracture point, after disruption of the bone tissue integrity and disintegration of blood vessels a formation of a hematoma occurs, immediately followed by an inflammatory response. After that, the fibrin blood clot with the inflammatory signaling molecules will form a temporary disorganized tissue to provide primary mechanical support and allow cell ingrowth, being the basis for the new bone formation. Subsequently, bone repair is initiated with the replacement of the hematoma by external soft tissues and cartilage. This biological phase is denominated as fibrocartilaginous callus formation, providing mechanical support and stabilization of the fracture site. Besides this, the soft callus is gradually remodeled and replaced by a bony callus where osteoprogenitor cells differentiate into osteoblasts and form a mineralized bone matrix. Bone remodeling, the final stage of the repair process, involves transforming the woven bone into lamellar bone at the center of the bony callus, providing the blood circulation and reestablishment of functional bone structure [4,7,14,30,31].

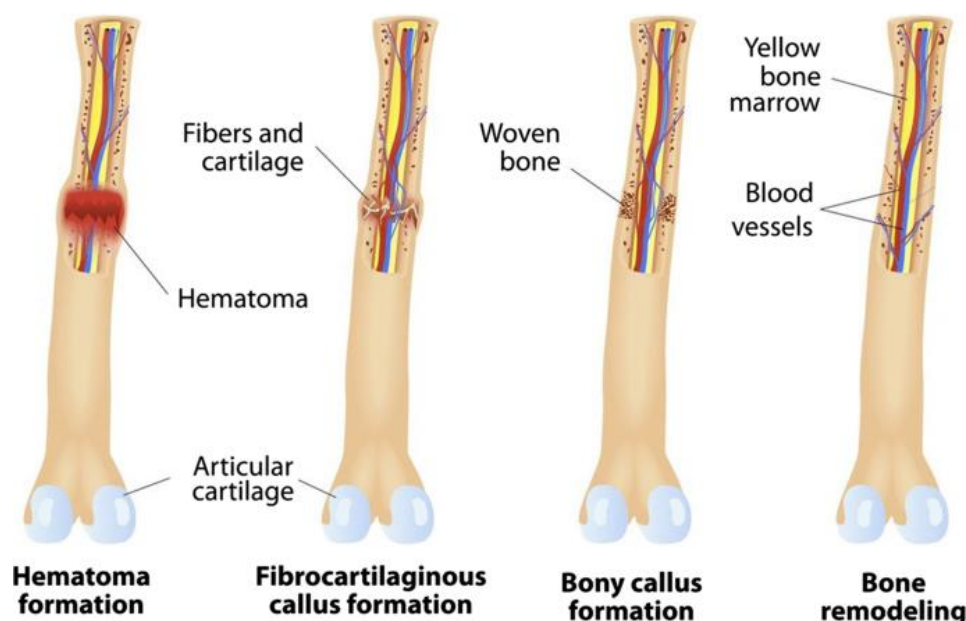


Figure 5- Stages of bone fracture healing mechanism [7].

2.2.5.1 Osteopontin in Bone Repair

Osteopontin (OPN) represents 1-2% of the non-collagenous proteins present in bone matrix consisting of about 300 amino acids. In bone, OPN is synthesized in the last stages of osteoblastic maturation, relating to time of matrix formation and it appears in high concentrations in the lamina limitans that underlies bone lining cells and also along the cement lines. Once the process of bone resorption is concluded osteoclasts also express OPN. The presence of OPN attracts osteoblasts to the bone resorption sites and promotes bone matrix deposition to fill the cavity. For this reason, OPN could also be used as a cytokine to mediate the attachment and communication between osteoblasts and osteoclasts [32-34].

OPN is a highly charged and phosphorylated protein characterized by having a fairly high affinity to calcium, modulating the nucleation of calcium phosphate during bone mineralization, and also by regulating the growth, shape and size of HA crystals [32,33,35]. Thus, OPN promotes fiber matrix bonding with the attachment of fibroblasts to plastic or glass substrates and fibronectin to collagen, thereby enhancing bone's resistance to fracture, as well as act as a bridge, in the case of microcracks formation where OPN inhibits crack propagation [18,32].

2.3 Bone Tissue Engineering

Tissue engineering is described as a multidisciplinary field of science that conjugates integrative approaches providing alternative strategies to improve or replace biological tissues. As a new area with a clinical prospect, bone tissue engineering (BTE) is based on the comprehension of bone structure, bone mechanics, and tissue growth. It is an emerging field that aims to overcome the limitations of conventional therapies, becoming a hopeful approach for bone regeneration. Biomaterials constructs such as 3D scaffolds play a crucial role for bone repair applications, mimicking the structure and function of the natural bone ECM, providing an environment to induce cellular adhesion, proliferation and differentiation, overcoming the current problems of replacing lost tissue function and boosting neovascularization and bone tissue regeneration [4,36-40].

2.3.1 Scaffolds

Scaffold's biomaterials can be described as a 3D temporary supporting framework structure able to mimic the natural tissue ECM in order to promote cell migration, adhesion, proliferation and matrix deposition forming a bone tissue-like substitute. This porous scaffold structure also allows the supply of nutrients, oxygen, removal of the cellular metabolism products, and controlled delivery of molecules of interest (drugs and growth factors). To promote higher pro-regenerative tissue response, there are several important requirements that scaffolds should follow. Below are described some important properties when designing or producing a scaffold for tissue engineering application [22,36,41].

I. Biocompatibility

Biocompatibility is a requirement of crucial importance in the selection of a scaffold for bone tissue engineering. The scaffold should replace the damage/loss of bone tissue, promote new tissue ingrowth and prevent specific immune reactions (such as antigen-antibody response) and severe inflammatory responses capable of reducing healing or causing rejection by the body. Hence, an ideal scaffold must have excellent biocompatibility to ensure cell survival and allow for successful integration into the host tissue without cytotoxicity effects [22,42].

II. Biodegradability

The aim of tissue engineering is to offer a non-permanent scaffold that acts as a cell delivery vehicle. Consequently, the scaffold must be biodegradable in a timely manner that allows the body's own cells to replace the implanted material by producing their own ECM.

Also, by gradually transferring loads, the 3D scaffold matrix should degrade at a similar rate of the tissue ingrowth. Thus, scaffold materials and their degradation products should not present toxic effects and be able to be removed from the body without interfering or causing damage to other organs or tissues [22,42].

III. Scaffold architecture

The scaffold architecture possesses a great importance once it is mandatory to have a 3D interconnected and highly porous structure to ensure cell adhesion and ECM deposition, as well as allow the flow of nutrients, oxygen and metabolic waste products removal. For bone tissue the average pore size of the scaffold is another key parameter and should follow a bimodal distribution (micro- and macroporous), being large enough to provide cell migration and neovascularization of the inner scaffold's architecture and also small enough to offer a sufficiently high surface area and favor protein adsorption [38,40,42].

IV. Mechanical properties

Scaffolds should be resistant enough to support surgical procedures and mechanical load immediately after implantation until the completion of the final remodeling process. Ideally, the scaffold should have mechanical properties consistent with the anatomical implantation site and possess a balance between mechanical properties and porous architecture to allow normal cellular function and vascularization [22,42].

2.3.2 Biomaterials

In BTE, two main categories of materials are used to produce scaffolds, including natural (organic), synthetic (artificial) materials with distinct scaffold structures that can be obtained from their materials' source, as showed at Figure 6. Each category of materials displays advantages and disadvantages. Metallic materials have higher mechanical properties when compared to the natural bone, causing stress shield which consequently lead to bone resorption, also presenting non-biodegradable behaviour [28]. Ceramic materials have been widely used for scaffold bone regeneration applications due to their excellent mechanical and physical properties (e.g. elastic modulus, compressive strength), bioresorbability (degradation rate), thermal stability and corrosion resistance. Nonetheless, some may cause chronic inflammatory response, low ductility (brittle materials) and questionable cell-matrix interaction. In comparison to synthetic polymers, natural polymers have as major advantages their similarity with the native ECM, biocompatibility, biodegradability and bioactivity. On the other hand, these materials may show uncontrollable degradation rate, and inadequate mechanical properties. Thus, the combination of polymers with bioceramics may result in composite structures with

enhanced biological response and mechanical behavior, which are fundamental properties for the scaffolds used in BTE [38,39,43].

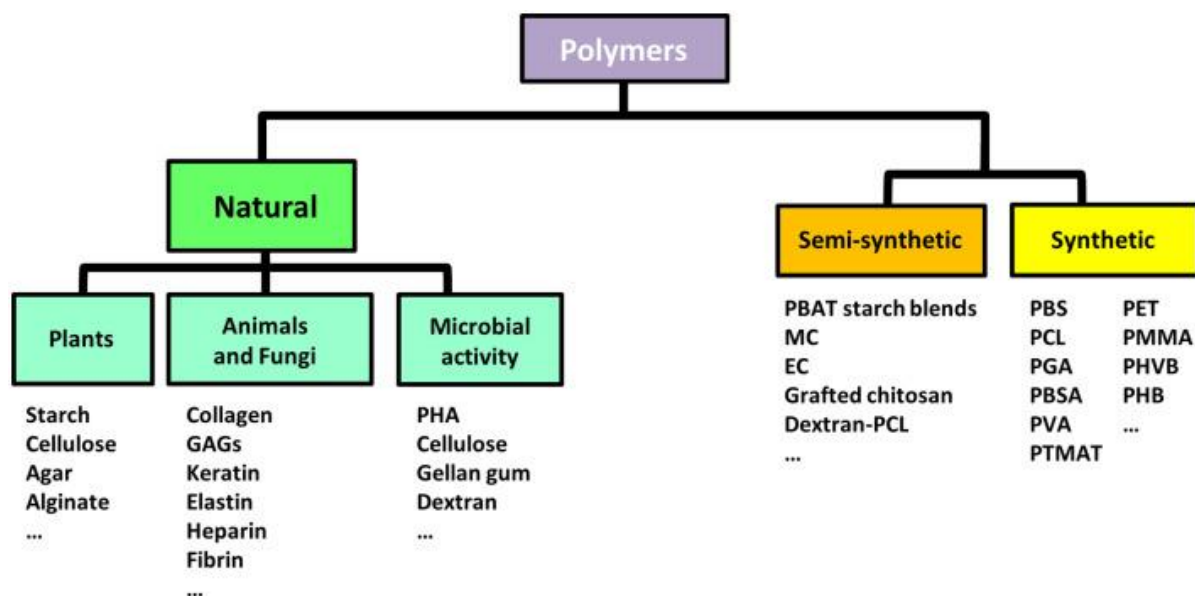


Figure 6- Classification of biodegradable polymers commonly used in biomedical applications based on their source (natural, synthetic, or semi-synthetic) [43].

2.3.2.1 Polymer/Bioceramic Scaffolds

Scaffolds made of ceramic materials are typically characterized by having a high mechanical stiffness (Young's modulus), very low elasticity, a hard and brittle structure. Bioceramics, such as HA, TCP, β -TCP and BGs, show excellent biocompatibility and have been commonly used in bone regeneration due to their chemical and structural similarity with the mineral phase (natural apatite) of the bone matrix. Furthermore, the interactions of bone cells with ceramics' surface favour an enhancement in osteoblast attachment, proliferation and overall implant osteointegration [28,38,42].

Recently, a newly developed nanocrystalline hydroxyapatite (10-100 nm) has been introduced in the composition of scaffolds and has received much attention because of its superior functional properties over its microscale counterpart, particularly higher surface reactivity and ultra-fine structure. Also, the presence of synthetic nanoHA in scaffolds is extremely advantageous since the bone has similar particle size within its natural structure. Those nanoparticles are also biocompatible, bioactive, biodegradable, osteoconductive, osteoinductive, nontoxic, non-inflammatory and a non-immunogenic agent and responsible to promote higher adhesion, proliferation and differentiation of progenitor cells, supporting bone ingrowth within a short period of time [11,12,28].

Despite its many advantages, pure nanoHA clinical applications for BTE has been limited because of its brittle characteristic, difficulty in shaping for implantation, and as the new bone is formed in a porous structure, HA network cannot sustain the mechanical loading needed for remodeling and it is restricted to low load-bearing applications. To overcome this limitation, nanoHA should be combined with a variety of other materials, such as collagen and reinforce the polymer matrix, mimicking the natural bone matrix [11,12,28].

Collagen is a natural polymer material that unlike scaffolds synthetically polymer-based usually promotes great cell adhesion and growth. Moreover, due to its binding capacity, it could be used in delivery systems for drugs, growth factors or cells. Therefore, collagen's biodegradability, solubility, tensile strength, mediation of intracellular interactions, stability, low immunogenicity and the possibilities for large-scale production, make it a significant biomaterial suitable for a widespread industrial use in orthopedic applications [44,45]. Nevertheless, pure collagen-based scaffolds have poor mechanical properties and are vulnerable to substantial gel contraction and unstable geometrical properties throughout cell culture [38,43].

Hence, in order to improve the mechanical and biological characteristics of the scaffold and achieve the ideal requirements needed, collagen and nanohydroxyapatite can be combined, increasing the mechanical properties, with a highly porous and interconnected structure, and also an improved permeability which benefits cell infiltration and subsequent vascularization. As a result, this highly porous biomimetic polymer/bioceramic composite scaffold offers a potential solution for BTE application [38,46].

2.3.3 Hydrogels in Bone Tissue Engineering

Hydrogels are described as a 3D network of crosslinked hydrophilic polymer chains, commonly referred to as a mesh, with 60-90% of water content that fills the space between the network of polymer chains and the centre of the larger pores. Under physiological conditions, the meshes hold the fluid and through expansion and contraction of the hydrogel an elastic force is imparted, being responsible for its solid soft consistency, analogous to living bone tissues [47-49]. The 3D physical integrity of hydrogels in aqueous conditions is guaranteed by chemical and/or physical crosslinking [50].

Hydrogels embody an ideal carrier for a wide range of applications in the bone tissue engineering field, once they are greatly used to transport cells and drug for controlled delivery promoting higher bone regeneration. Also, they have low cytotoxicity, desirable biodegradability, biocompatibility, can be sterilized, sorption capacity, injectable capability, low interface tension with aqueous media, swelling/deswelling behaviour, high ionic conductivity, high permeability and high environmental sensitivity [47,48,50-52].

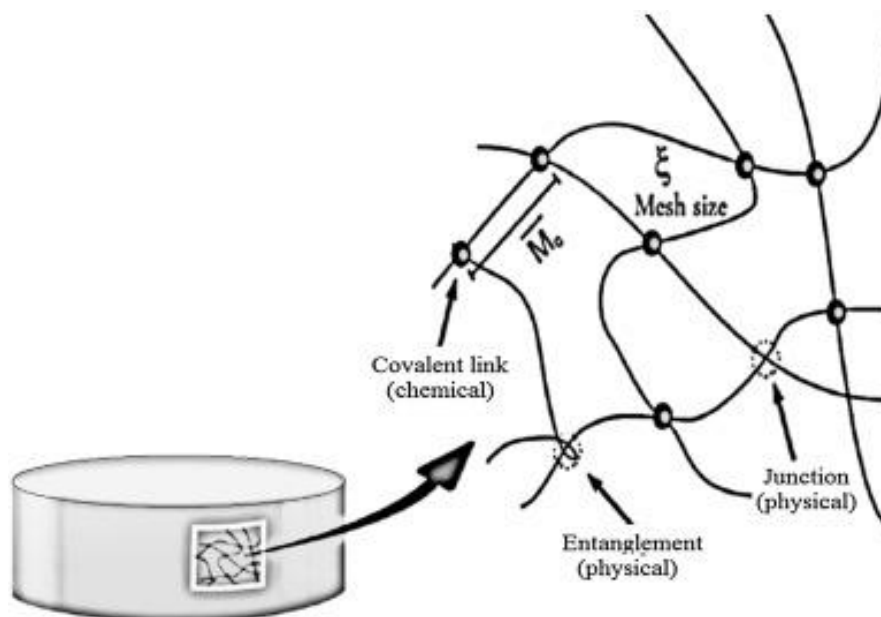


Figure 7- Hydrogel chemical structure representation [48].

2.3.3.1 Classification of Hydrogels

Hydrogels' classification depends on their physical properties, polymeric composition, method of preparation, nature of swelling, network ionic charges, biodegradation rates and type of cross-linked bonding [44,48]. They can be designed from a wide variety of material sources, from totally synthetic to natural, expanding their versatility. Natural hydrogels are proteins or polysaccharides derived from biological resources, such as collagen, albumin, gelatin, fibrin, hyaluronic acid, chitosan, dextran, agarose, and alginate. These materials have good biocompatibility, biodegradability, low immune response and are non-toxic, resembling native bone structures. Furthermore, hydrogel natural constructs allow cell adhesion, proliferation, differentiation and new tissue regeneration, being absorbed through a metabolic or enzyme-controlled degradation. Nevertheless, like any other natural material, there are some drawbacks such as low reproducibility, stability, poor mechanical strength and stiffness [44,49-51].

Synthetic hydrogels biomaterials are prepared through chemical reactions, showing a defined structure, long shelf stability, reproducibility and large-scale production. However, they possess poor biocompatibility and bioactivity, when compared to natural materials and therefore, synthetic hydrogels could be used blended with natural materials and chemical clues to compensate each of those disadvantages and to offer a hydrogel with increased biological response [44,50].

2.3.3.2 Fibrin-based Hydrogel

Fibrin is described as a natural fibrous protein which possesses distinguished advantages derived from their exclusive biological and physical properties, being an excellent candidate for tissue engineering field applications [51-54]. Immediately after an injury occurs, the coagulation cascade initiates and the clotting enzyme thrombin induces polymerization of soluble fibrinogen into an insoluble fibrin mesh, which alongside with platelets form a blood clot. This 3D fibrin scaffold acts as a temporary structure for cells, establishing hemostasis and also deposition of a new ECM, being critical in wound healing repair. Furthermore, fibrin contains numerous specific bonding sites for cell–matrix interactions promoting cell infiltration, fibroblast proliferation and angiogenesis. Fibrin-based hydrogels also have the advantage of being an excellent biocompatible fully injectable hydrogel, capable of filling any shape or geometry gaps. However, low mechanical properties and high enzymatic degradation rate are the major disadvantages of fibrin hydrogels [49,53-55].

Fibrin is the polymer of fibrinogen molecules, naturally present in blood plasma and is composed of two sets of three different polypeptide chains, namely $\text{A}\alpha$, $\text{B}\beta$, and γ . When the thrombin-mediated cleavage of the *N*-terminal fibrin peptide is completed, a branching of fibrin protofibrils is synthesized and then a 3D network of fibrin strands is formed. The originated structure is inherently weak, however its long-term stability, structure, and mechanical strength can be enhanced through different methods such as modification of fibrinogen, Ca^{2+} and thrombin concentrations, proteins incorporation, temperature, pH, and crosslinking agents (e.g., fibronectin or factor XIII). Therefore, highly concentrated thrombin and fibrinogen environments result in thin fibres with many branching points and a geometry with small pore size, leading to a less porous and permeable matrix for oxygen and nutrients diffusion and cell viability. Although, lower thrombin concentrations are associated with shorter gelation times, resulting in thick fibres with low branching points and larger pores, offering a highly porous network. Biologically, the high porous network has a direct impact on the cellular response. Studies suggest that low fibrinogen concentrations lead to an increase in cell proliferation, while high fibrinogen concentrations promote an increase in cell differentiation. Nevertheless, higher contents of fibrinogen lead to a decrease in final mechanical properties [49,53,54].

2.3.3.3 Fibrin-based Hydrogel in Bone Tissue Engineering

In bone tissue engineering, fibrin-based hydrogels arise as potential solutions for healing injured tissues not only due to their critical homeostatic properties, but also through the enhancement of the initial mechanical support that will allow angiogenesis, and subsequently the promotion of cell infiltration and long-term tissue remodeling. In addition, in wound repair, fibrin reduces blood loss, establishes a barrier against microbial infection,

and offers a biodegradable autologous scaffold, crucial in cell activity during the defect repair. Thus, fibrin-based hydrogels can have applications for bone tissue engineering applications as a delivery vehicle for cells, antimicrobial agents and growth-factors, or as injectable fibrin polymerized within scaffolds, films or thin layers to repair defect problems [54,56].

2.3.4 Cells

A successful approach in tissue engineering implies the combination of three pillars: (a) cells (stem cells or progenitor cells), representing the essential structural unit of any tissue that will be responsible for synthesizing the new tissue matrix; (b) biological factors (GF/ BMPs) to guide cellular activity and promote tissue formation; and (c) an ECM support such as scaffolds, as material structure necessary for cell adhesion, proliferation and differentiation. Vascularization is also a key element in providing oxygen and nutrients for the cells' viability, and to remove waste products [57,58].

2.3.4.1 Human Dental follicle Stem Cells (hDFSCs)

Synthetic bone scaffolds seeded by multipotent stem cells are widely used in bone tissue regeneration due to their capability of mimicking biological processes. The mesenchymal stem cells (MSCs) are progenitors with clonogenicity, multi-lineage differentiation and self-renewal capability. In literature, MSCs can be found in a number of adult tissues, including bone marrow, adipose tissue, peripheral blood, muscle, skin, intestine, endometrium, pancreas, brain and hair follicles, as well as in various oral donor tissues, for example deciduous elements, the periodontal ligament, the dental follicle, dental pulp, apical papilla and gingival tissue [6,57,59,60].

The source of MSCs has a crucial role in the outcomes of BTE, therefore, in recent years, the easy accessibility and harvest, high proliferation capacity, and multidirectional regenerative potential make hDFMSCs an important source of MSCs for clinical applications in BTE. hDFMSCs are typically isolated from the dental follicle of human third molars, which is a loose ecto-mesenchyme-derived connective tissue sac surrounding the developing tooth germ prior to eruption. These spindle-shaped cells possess the capacity for non-limited self-renewal and multipotent potential to differentiate into mesodermal, ectodermal, and endodermal lineages, including, odontoblasts, cementoblasts, periodontal ligament cells, osteoblasts, chondroblasts, epithelial cells, adipocytes, vascular cells, neuronal cells and muscle cells. Thus, DFSCs combined with 3D-engineered scaffolds show excellent regenerative capabilities, via the release of osteogenic growth factors and stimulation of the migration and differentiation of host osteoprogenitors, providing a new therapeutic approach to improve the formation of new bone and osteointegration [6,39,57,60].

CHAPTER 3

Materials and Methods

Chapter 3- Materials and Methods

3.1 Materials

Collagen type I from Achilles's tendon bovine, phosphate buffered saline (PBS), Human Osteopontin (OPN), p-nitrophenol phosphate, trypsin EDTA, paraformaldehyde (PFA), Triton X100, 4'-6-diamidine-2-phenylindole (DAPI), sodium hydroxide (NaOH), sodium chloride (NaCl), potassium chloride (KCl), hydroxymethyl aminomethane (TRIS), β -glycerophosphate, dexamethasone and tris-phosphate buffered saline (TBS) were purchased from Sigma-Aldrich (St. Louis, USA). Hydrochloric acid (HCl), 1-ethyl-3-(3-dimethyl aminopropyl) carbodiimide hydrochloride (EDC), N-hydroxysuccinimide (NHS) and rabbit anti-human Osteopontin (AB 1870, 1:500) were obtained from Merck (Germany). Nanohydroxyapatite aggregates (nanoHA- nanoXIM.HAp202) was provided from Fluidinova S.A (Maia, Portugal). Fetal bovine serum (FBS), penicillin and streptomycin were provided from Gibco (Waltham, Massachusetts, USA). Culture cell medium Dulbecco's Modified Eagle Medium (DMEM) was acquired from HyClone. Quant-iT™ Picogreen® DNA assay kit, Thermo Scientific™ Pierce™ BCA Protein Assay Kit, Alexa Fluor-conjugated Phalloidin 594 nm and Alexa Fluor 488 goat anti-rabbit IgG secondary antibody were purchased from Invitrogen (Molecular Probes, USA). Vectashield was acquired from Vector laboratories (United Kingdom).

3.2 Fibrin Hydrogel (with and without OPN)

3.2.1 Preparation of Fibrin Hydrogel

A Fibrinogen solution (Fb) was obtained by dissolving in Tris-buffered saline (TBS) was prepared by mixing 134 mM of NaCl, 2.7 mM of KCl and 33 mM TRIS, pH 7.4, in a concentration of 20 mg/ml (30 μ L/scaffold)). A work solution containing thrombin (Tb) and CaCl_2 [final concentration of 2 National Institute of Health (NIH) U/ml thrombin from human plasma; 2.5 mM CaCl_2] was prepared for a final volume of 60 μ L/scaffold. After cell loading, Fb was gently mixed in a proportion of 1:2 with the Tb/ CaCl_2 work solution. The fibrin gel crosslinking was induced at a 37°C incubator with a CO_2 atmosphere for 30 minutes.

3.2.2 Preparation of OPN

Human Osteopontin (OPN, recombinant, expressed in NSO cells, $\geq 95\%$ (SDS-PAGE), Merck, France)) solution was obtained by dilution in tris-phosphate buffered saline (TBS) with pH of 7.4, at concentration of 100 μ g/mL.

3.2.3 Preparation of Fibrin - OPN Hydrogel

The OPN solution (10 μ L of 100 μ g/mL solution) was initially mixed with a fibrinogen solution (20 mg/mL) before adding it to the thrombin/ CaCl_2 and cells solution (final concentrations: 6.3 mg/mL of Fb, 2 NHI U/mL of Tb, 2.5 mM of CaCl_2 , 10 μ g/mL of OPN and cells).

3.3 *In vitro* biological studies

3.3.1 Establishment of Stem Cell Cultures from the Human Dental Follicle (hDFMSC)

Previously, human dental tissues fragments (follicle tissue) were obtained, digested and hDFMSCs were isolated by adherent culture on plastic tissue culture substrates. After confluence, cells were separated and characterized by flow cytometry and qPCR analysis [61]. Human follicle MSCs were cultured in a basic cell culture medium and kept at 37°C in a 5% carbon dioxide (CO_2) atmosphere.

3.3.2 Cell Culture

Human osteoblast-like cells (MG63; ATCC) and human dental follicle mesenchymal stem cells (hDFMSC; isolated from patient tissue) were cultured in Dulbecco's Modified Eagle Medium supplemented with 10% fetal bovine serum (FBS) and 1% penicillin-streptomycin (3×10^4 mol/L and 5×10^4 mol/L), maintained at 37°C and 5% of carbon dioxide (CO_2). After cell confluence of 90% on T flask (75 cm^2 ; Nunc), cells were washed with PBS solution, detached with trypsin solution (0.5%) at 37°C for 5 min, and counted using a Neubauer chamber. Cells were loaded into the hydrogel in a concentration of 1.5×10^5 cells/scaffolds.

3.3.3 Cellular Proliferation Assay

DNA content was measured using the Quant-iT™ Picogreen® DNA assay according to the manufacturer's instructions. After each time-point, scaffolds were washed with PBS and then incubated with 0.5 ml of ultra-pure water at 37°C and 5% CO_2 for 1 h. Subsequently, scaffolds were placed in a freezer at -20°C until the end of the experiment and then thawed at room temperature to lyse all the cells membranes. The scaffolds were

cut into pieces with a scissor and vortexed for 20 seconds, after that, the solution was centrifuged with 2000 rpm for 5 min. The supernatant with the lysed cells was collected (20 μ l) and incubated with Picogreen® solution. Lastly, the fluorescence intensity was measured with a microplate spectrofluorometer (SynergyMx, BioTek) at 480 and 520 nm excitation and emission, respectively. The results were expressed in nanograms of DNA per milliliter.

3.3.4 Cellular Differentiation Assay and Protein Quantification

The alkaline phosphatase activity (ALP) was measured as quantitative analysis for early osteogenic characterization. The same supernatant with the lysed cells obtained as described above (Subsection 3.3.3) was used for the enzyme activity and total protein content protocol. The ALP enzyme activity was followed through substrate hydrolysis, using p-nitrophenol phosphate, in alkaline buffer solution, (pH=10). After 1 hour of incubation, at 37°C, the reaction was suspended by adding NaOH (0.02 M) and the p-nitrophenol was quantified by absorbance at 405 nm, using a plate reader (Synergy MX, BioTek). Lastly, the ALP results were expressed in nanomoles (nmol) of p-nitrophenol produced per minute (min). The ALP activity results were normalized to total protein content and were expressed in nanomoles of p-nitrophenol produced per minute per mg of protein. Total protein content was measured by Lowry's method (Thermo Scientific™ Pierce™ BCA Protein Assay Kit) with bovine serum albumin used as standard. Results were expressed in milligrams of protein concentration per milliliter.

3.3.5 Confocal Laser Scanning Microscopy (CLSM)

Two samples from each time-point were fixed with 4% paraformaldehyde and incubated for 30 min at room temperature. After that, the materials were incubated with 0.1% Triton X100 solution for 30 min at room temperature and then washed twice with 1% bovine serum albumin (BSA) in PBS. The samples were then incubated for 1 hour into BSA solution. The cells' cytoplasm (actin fibers) was stained with Alexa Fluor-conjugated Phalloidin 594 nm (dilution of 1:200) for 1 h at room temperature and under darkness and nuclei were stained with DAPI (4'-6-diamidine-2-phenylindole at 0.2%) for 5 min.

For human osteopontin immunostaining, identical protocol was performed for the cell membrane's permeabilization and to block non-specific binding as described above. Samples were then incubated with rabbit anti-human Osteopontin (AB 1870, Merck, Portugal, 1:1000) overnight at 4°C. This procedure was followed by 1 h incubation with Alexa Fluor 488 goat anti-rabbit IgG secondary antibody (1:1000). Samples were subsequently washed and nuclei were counterstained with 1 μ g mL⁻¹ DAPI for 10 min at room temperature. All samples were covered by Vectashield. Images were acquired with

excitation lasers of 405, 488 and 594 nm and evaluated by Confocal Laser Scanning Microscopy (CLSM, Leica SP2 AOBS SE camera).

3.3.6 Statistical Analysis

Data were presented as mean and standard deviation, and they were analysed using the two-way ANOVA test (GraphPAD software). Differences between groups and time-points were considered statistically significant when $p < 0.05$.

3.4 Preparation of Collagen/nanohydroxyapatite Scaffolds

Coll/nanoHA scaffolds were obtained from the cryogelation technique. Initially type I insoluble collagen was swelled overnight in 10 mM chloride acid (HCl) solution at 4°C at a concentration of 2 % (w/v). Then, the dispersion was homogenized (Ultra Turrax T25, IKA) at 11000 rpm for 1 h.

Coll/nanoHA composite cryogel was set with 5 ml of collagen slurry diluted in 4.5 mL of HA (nanometric), suspended in 10 mM chloride acid (HCl). The dry powder of HA (nanoparticles) were mixed with the chloride acid solution in a specific ratio (2%) and vortex to homogenize (final composition Coll/nanoHA 50:50).

For the preparation of cryogels, 20 mM NHS and 40 mM EDC were added to the collagen slurry and promptly transferred to a syringe (5 ml) that was used as a mold. This solution was kept in a freezer at -18°C for 24 hours to conclude the crosslinking.

Lastly, the scaffold was thawed at room temperature and, afterwards, the samples were washed with distilled water. The samples were frozen overnight at -80°C and dried with a freeze-dryer (Labconco, FreeZone 6) at 0.1 bar for 24 h. The Coll/nanoHA samples were cut with a surgical blade with 4 mm width.

3.5 Preparation of Coll/nanoHA - Fibrin Hydrogel composite

The Coll/nanoHA cryogel scaffolds were produced as described above and cut into discs (10 mmx4 mm). In some samples, the fibrin hydrogel (with and without OPN) with a total of 1.5×10^5 cells/scaffold (MG63 or hDFMSC) were gently pipetted up and down within each scaffold. As a control, both cell types were centrifuged and concentrated in a small volume (1.5×10^5 cells/10 μ l) and dropped into the scaffold. Subsequently, the scaffolds were placed inside a non-tissue culture 24-wells plate for 30 minutes at a standard

incubator (37°C, 95% humidified air and 5% v/v CO₂) to allow cell adhesion and hydrogel crosslinking.

Afterwards, the wells were filled (1 mL) with basic cell culture medium and incubated at time-points of 3, 7, 14 and 21 days. This osteoinductive cell culture medium was prepared with Dulbecco's Modified Eagle Medium with 10% FBS, 1% P/S, 10 mM of β - glycerophosphate and 0.1 mM of dexamethasone (Appendix B). The osteoinductive medium was added after 3 days of scaffolds incubation. The both cell culture mediums were changed every 3 days.

These experiments were aimed at evaluating MG63 and hDFMSC cells proliferation and differentiation within the biomaterials, measuring the cells DNA concentration and the alkaline phosphate activity (osteogenic differentiation).

CHAPTER 4



Results

Chapter 4- Results

4.1- *In vitro* Biological Studies: MG63

4.1.1- DNA Quantification Assay

MG63 cells proliferation rate within Coll/nanoHA_Fb, Coll/nanoHA_Fb-OPN, and Coll/nanoHA 3D scaffolds, was assessed by DNA quantification and it is shown in Figure 8. It is worth noticing the rise in the DNA concentration within Coll/nanoHA_Fb and Coll/nanoHA samples along the time. The two-way ANOVA test statistical analysis was performed for all the samples and no statistical differences were noted among different samples at the same time-point. Furthermore, Coll/nanoHA_Fb-OPN scaffold showed increase of DNA content after 7 and 14 days.

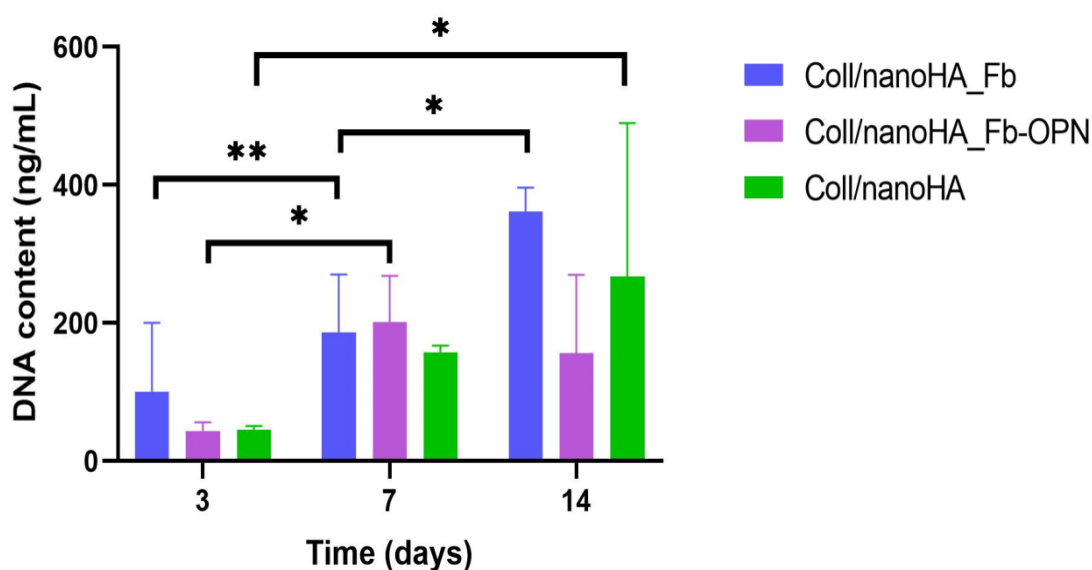


Figure 8- Total DNA content of MG63 cells within Coll/nanoHA_Fb, Coll/nanoHA_Fb-OPN, and Coll/nanoHA biocomposite scaffolds after 3, 7 and 14 days of culture in basic medium. Statistical differences between samples from different time-points, * $p < 0.05$ and ** $p < 0.01$.

4.1.2- Total Protein Content

Figure 9 shows the total protein content for MG63 cultured within Coll/nanoHA_Fb, Coll/nanoHA_Fb-OPN and Coll/nanoHA, during 3, 7, and 14 days. Total protein content showed high increase within Coll/nanoHA_Fb-OPN composite scaffold after 7 and 14 days. Coll/nanoHA_Fb biocomposite protein content also showed a tendency to increase with

time, as opposed to Coll/nanoHA scaffold that showed a tendency to decrease. Moreover, the highest protein concentrations were observed for Coll/nanoHA_Fb-OPN scaffold in the time span following 14 days of culture.

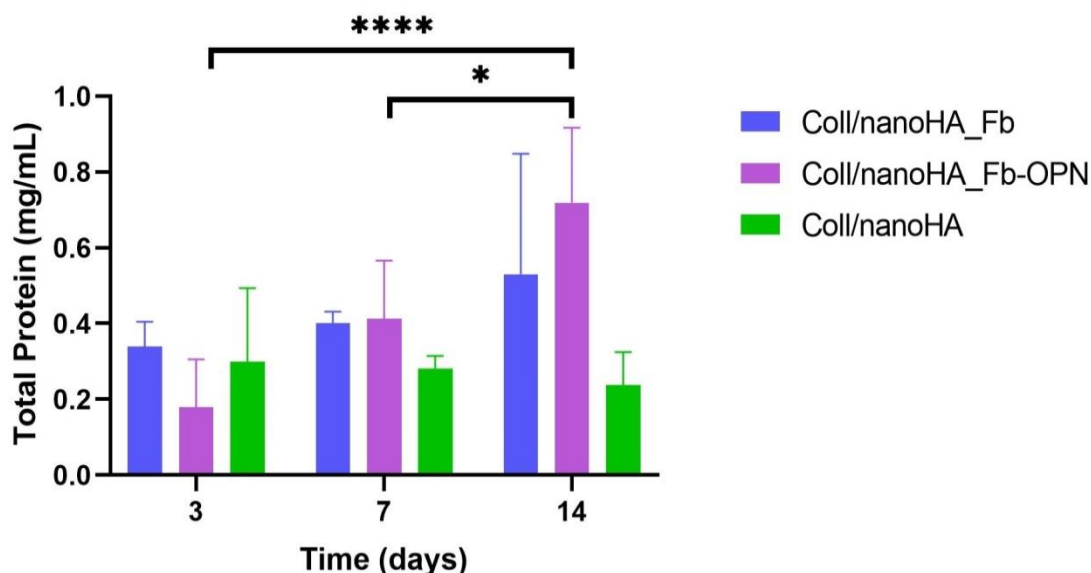


Figure 9- The total protein concentration for MG63 cells (ECM) within Coll/nanoHA_Fb, Coll/nanoHA_Fb-OPN, and Coll/nanoHA biocomposite scaffolds after 3, 7 and 14 days of basic culture. Statistical differences between samples from different time-points, *p < 0.05 and ****p < 0.0001.

4.1.3- Alkaline Phosphatase (ALP) Activity

The assessment of ALP activity was conducted with osteoblast-like cells (MG63) following 3, 7 and 14 days of culture within Coll/nanoHA_Fb, Coll/nanoHA_Fb-OPN, and Coll/nanoHA composite scaffolds. ALP is a quantitative criterium of early cell differentiation, and is consequently, an early sign of osteoblastic phenotype [62]. As shown in Figure 10, Coll/nanoHA_Fb-OPN was the sample with the highest enzyme activity after 3 days. However, after day 7 and day 14, ALP activity showed a slight decrease. Thus, the ALP activity was slightly higher for Coll/nanoHA_Fb-OPN scaffold in comparison to other samples, but the statistical test did not show any differences among samples and time-points (two-way ANOVA – p > 0,05).

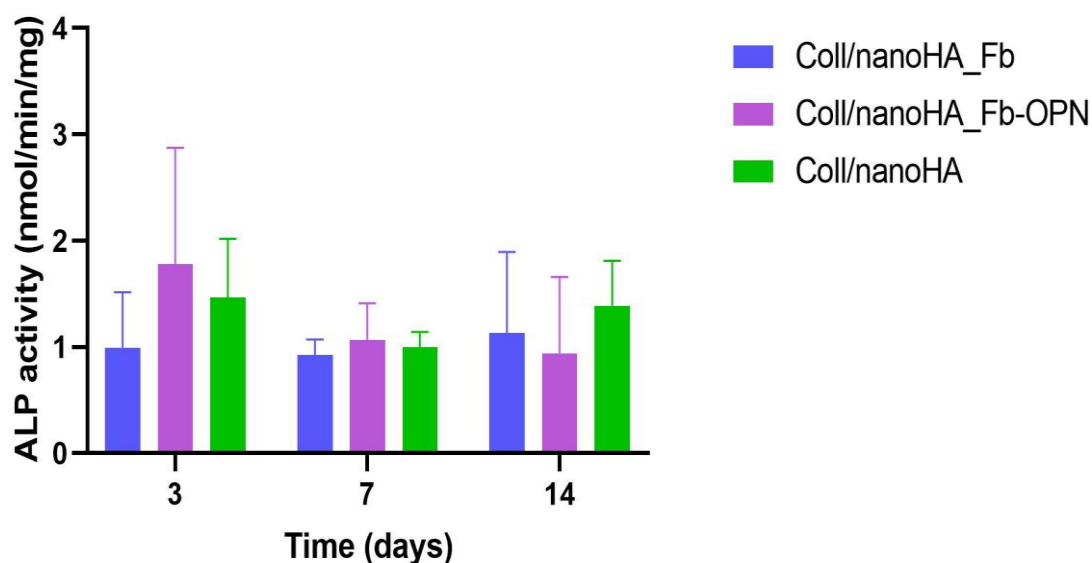


Figure 10- ALP activity of MG63 osteoblast-like cells culture within Coll/nanoHA_Fb, Coll/nanoHA_Fb-OPN, and Coll/nanoHA biocomposite scaffolds after 3, 7 and 14 days of culture. Statistical differences ($p > 0.05$) were not observed.

4.1.4- Confocal Laser Scanning Microscopy

The morphology and the human proteins secreted by MG63 cells were evaluated by the immunostaining of human OPN and cytoplasm actin (phalloidin) within Coll/nanoHA_Fb and Coll/nanoHA_Fb-OPN biocomposite scaffolds after 3, 7 and 14 days of culture. CLSM images on Figure 11 show that OPN protein is well distributed within all the Coll/nanoHA_Fb-OPN scaffold. Besides, the presence of OPN was more evident on the periphery of the OPN- modified scaffolds which seemed to follow the irregularities of the materials' surfaces in accordance with the higher number of cells covering this pore walls' area, when compared to Coll/nanoHA scaffold without OPN. Furthermore, CLSM images also corroborate that the scaffolds without OPN had fewer cells when compared to scaffolds with OPN. Hence, MG63 cells cultured within Coll/nanoHA_Fb-OPN secreted ECM with higher presence of human OPN on the material's surface.

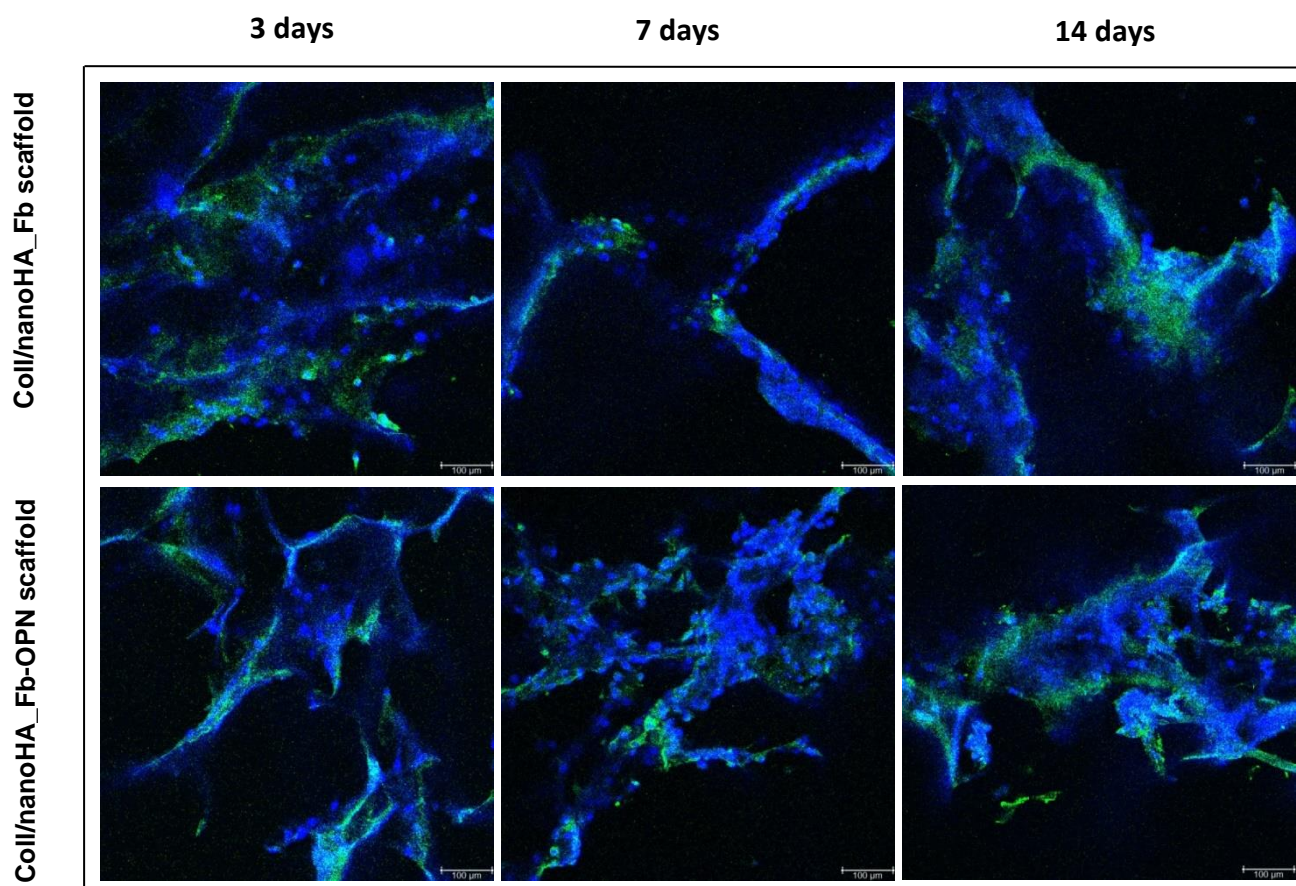


Figure 11- CLSM images showed the human ECM (osteopontin) of MG63 after 3, 7 and 14 days of culture within Coll/nanoHA_Fb scaffold (with and without OPN). MG63 nuclei were stain in blue and human OPN in green. Scale bar: 100 μ m.

MG63 osteoblast-like cells normal morphology and distribution on Coll/nanoHA is shown at Figure 12 [63]. The cells presence within Coll/nanoHA_Fb and Coll/nanoHA_Fb-OPN biocomposite scaffolds were observed using CLSM after 3, 7 and 14 days of culture. In Figure 13, it is possible to observe that the cell ingrowth seems to follow the irregularities of the materials' surface, covering the pore walls of both scaffolds. At day 14, both biocomposite scaffolds surfaces and macropores walls were almost completely covered by cells that formed continuous cell layers in some regions. Besides that, it should be observed that at this time-point the Coll/nanoHA_Fb-OPN scaffold show the highest cell viability and density. Also, cells in two different morphologies can be distinguished: one spread and well adhered, entirely covered the scaffolds surfaces in early stages of culture and another round and agglomerated, at the late stage of culture. Furthermore, within Coll/nanoHA_Fb-OPN scaffold, MG63 cells start to aggregate and present a less spread distribution.

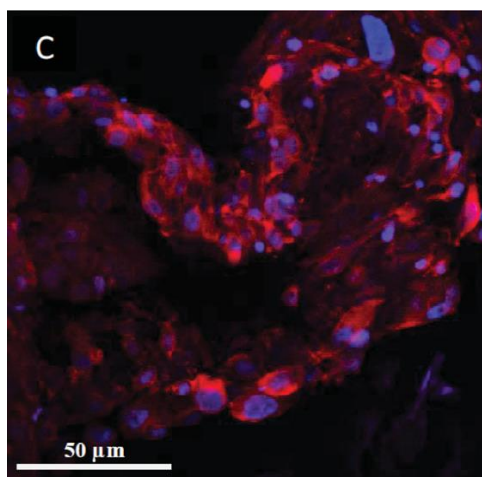


Figure 12- CLSM image of MG63 osteoblast-like cells cultured within Coll/nanoHA (50:50) biocomposite scaffolds after 21 days of culture (normal morphology). Image courtesy of [63].

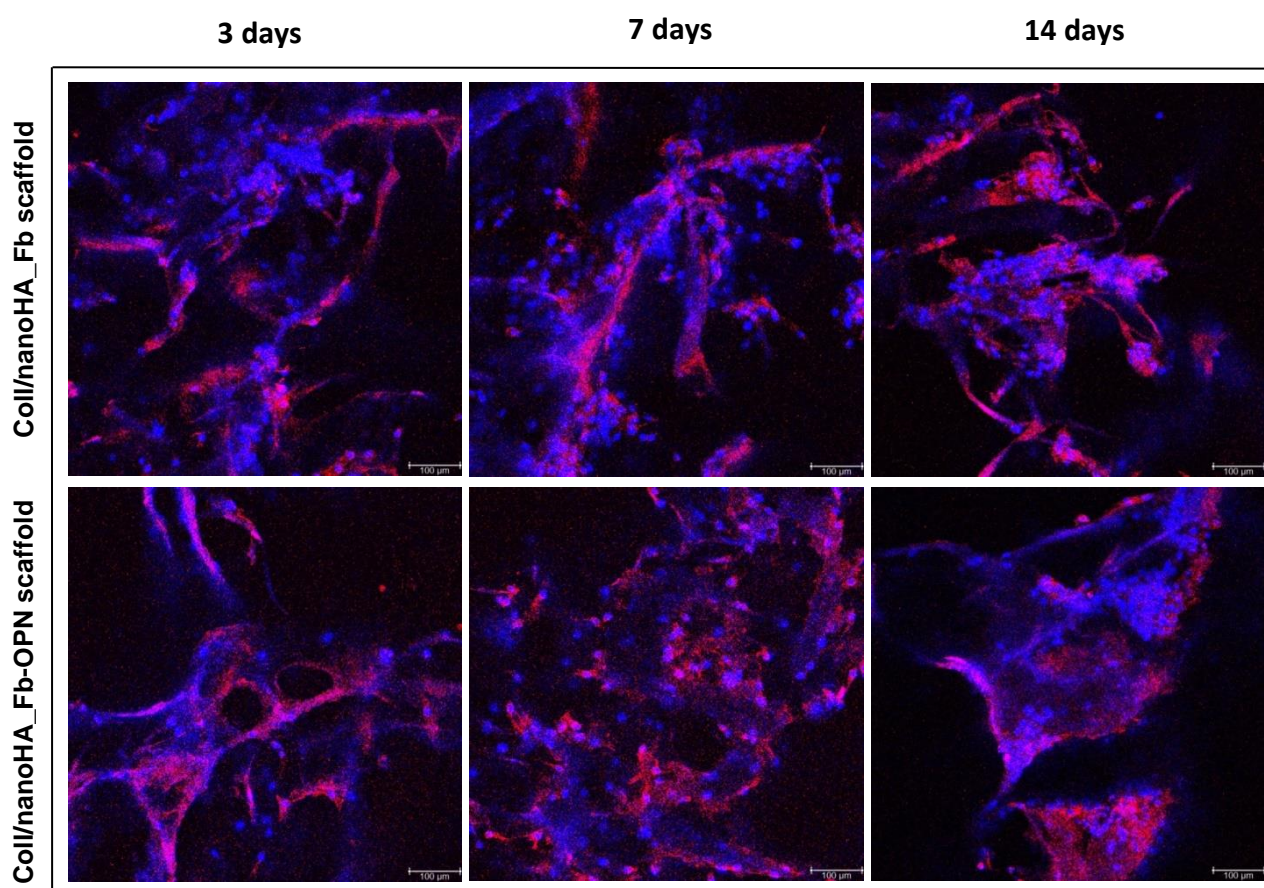


Figure 13- CLSM images showed the morphology of MG63 after 3, 7 and 14 days of culture within a Coll/nanoHA_Fb scaffold (with and without OPN). MG63 nuclei were stain in blue and cytoplasm (actin filaments) in red. Scale bar: 100 μm.

4.2- *In vitro* Biological Studies: hDFMSCs

4.2.1- DNA Quantification Assay

hDFMSCs proliferation rate on Coll/nanoHA_Fb, Coll/nanoHA_Fb-OPN, and Coll/nanoHA 3D composite scaffolds, estimated by DNA extraction quantification is showed in Figure 14. It was possible to observe that hDFMSCs exhibited the highest overall proliferation rates in Coll/nanoHA_Fb-OPN biocomposite in comparison to other samples. Moreover, after 14 and 21 days of culture total DNA content was three and two fold higher, respectively, when compared to 7 days of culture. Different proliferation rate was observed in Coll/nanoHA_Fb with a decrease in the DNA concentration from day 7 to day 14 of culture. In the same material, from day 14 to 21 a slight increase was noticed, although it was not statistically different. Coll/nanoHA scaffold show similar results during all time of culture, with non-statistical differences, but a slightly increase is observed in the total DNA content from day 14 to 21.

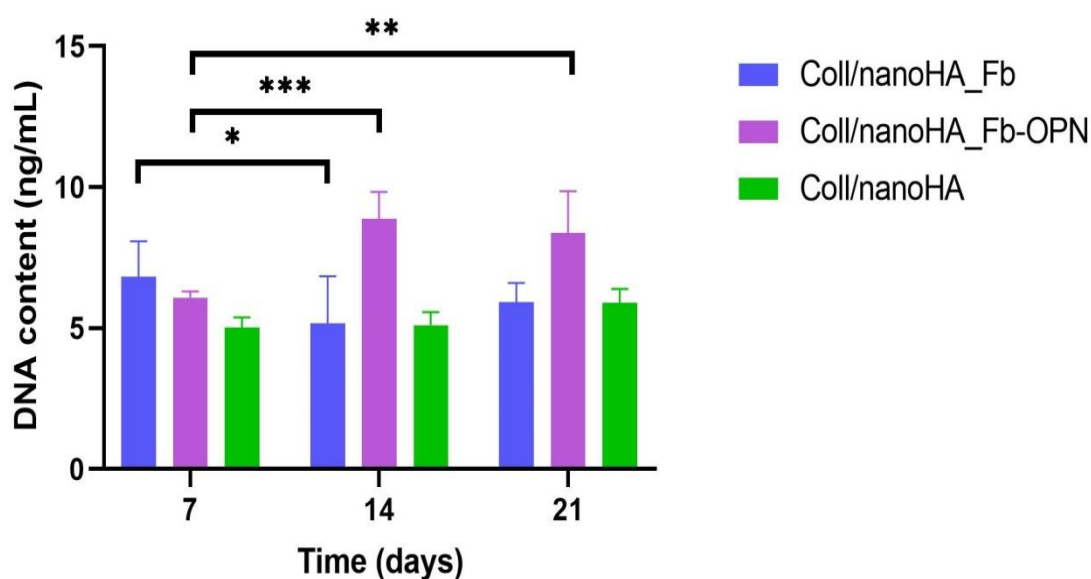


Figure 14- Total DNA content expression of hDFMSCs proliferation rate in Coll/nanoHA_Fb, Coll/nanoHA_Fb-OPN, and Coll/nanoHA biocomposite scaffolds for 7, 14 and 21 days of culture in basic medium. Statistical differences between samples from different time-points, *p < 0.05, **p < 0.01 and ***p < 0.001.

4.2.2- Total Protein Content

The total protein content of Coll/nanoHA_Fb, Coll/nanoHA_Fb-OPN and Coll/nanoHA scaffolds with hDFMSCs cultured for 7, 14, and 21 days is shown in Figure 15. Statistical differences were observed between Coll/nanoHA_Fb and Coll/nanoHA from day 7 to 21 and Coll/nanoHA_Fb-OPN for all time points. Moreover, higher protein concentrations were observed within the Coll/nanoHA_Fb-OPN scaffold presenting a peak at day 14, followed by a decrease at later time-point. Coll/nanoHA_Fb and Coll/nanoHA biocomposite scaffolds showed a decrease of the total protein content from early time-points of culture (7 days) to the later ones (21 days).

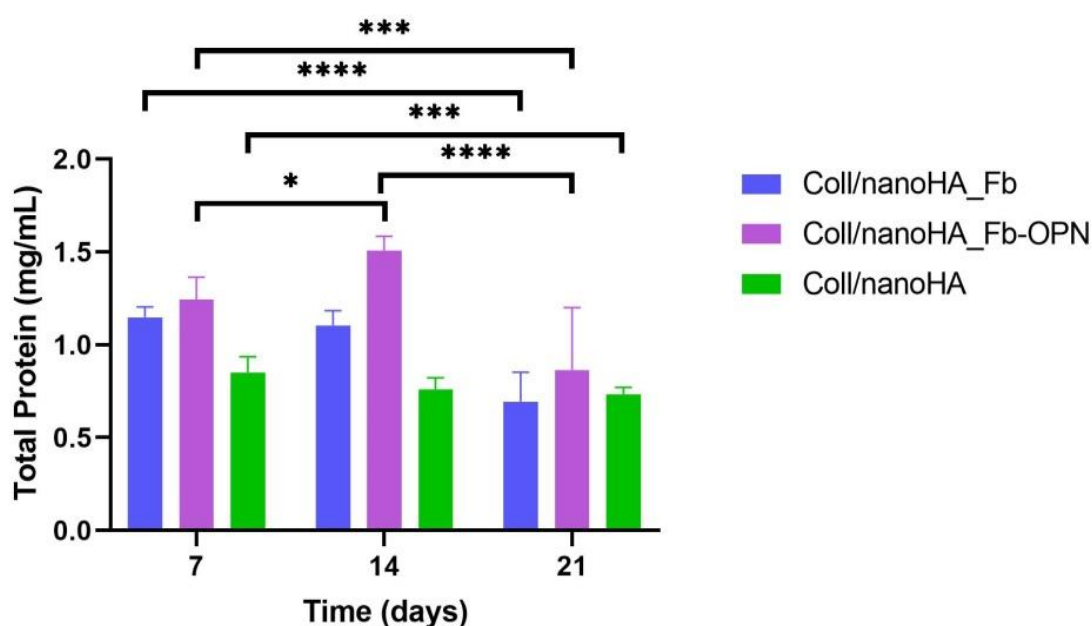


Figure 15- The total protein secreted by hDFMSCs (ECM) in Coll/nanoHA_Fb, Coll/nanoHA_Fb-OPN, and Coll/nanoHA biocomposite scaffolds after 7, 14 and 21 days of culture. Statistical differences between samples from different time-points, *p < 0.05, *** p < 0.001 and ****p < 0.0001.

4.2.3- Alkaline Phosphatase (ALP) Activity

The osteogenic differentiation of hDFMSC within Coll/nanoHA_Fb, Coll/nanoHA_Fb-OPN, and Coll/nanoHA biocomposite scaffolds was assessed by measuring the ALP activity after culture for up to 21 days. ALP is present as a membrane marker of all types of stem cells and it is also an earlier marker of osteogenic differentiation. The two-way ANOVA statistical test was performed for the different samples and time-points, as shown in Figure 16. Statistical differences of ALP activity were observed for hDFMSCs cultured within Coll/nanoHA_Fb-OPN biomimetic scaffold and showed an increase of the enzyme activity after 7 days, regarding an early stage of differentiation, and after 21 days regarding

a later osteogenic maturation. Coll/nanoHA and Coll/nanoHA_Fb samples followed the same pattern, although Coll/nanoHA_Fb 3D composite scaffold showed a small decrease of ALP activity at day 14.

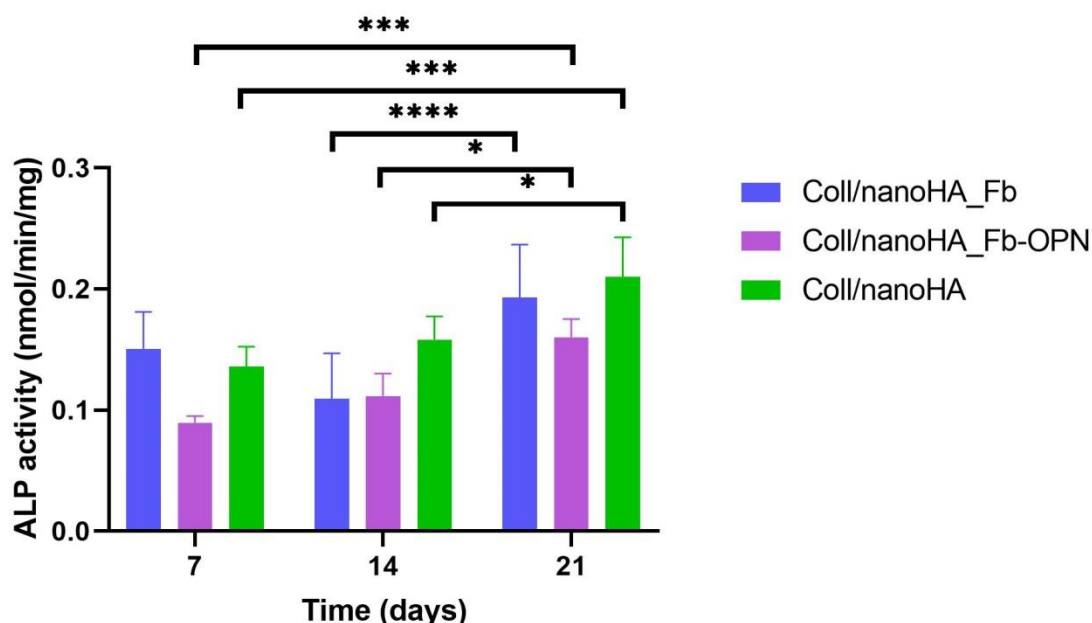


Figure 16- ALP activity of hDFMSCs cultured within Coll/nanoHA_Fb, Coll/nanoHA_Fb-OPN, and Coll/nanoHA biocomposite scaffolds after 7, 14 and 21 days. Statistical differences between samples from different time-points, *p < 0.05, *** p < 0.001 and ****p < 0.0001.

4.2.4- Confocal Laser Scanning Microscopy

The cellular morphology and the human proteins secreted by hDFMSCs were evaluated by the staining of cell actin cytoplasm and human OPN within Coll/nanoHA_Fb, Coll/nanoHA_Fb-OPN and Coll/nanoHA biocomposite scaffolds after 7, 14 and 21 days of culture. CLSM images at Figure 17 show that in Coll/nanoHA_Fb-OPN scaffold, hDFMSCs presented in early stages of cell culture are spread and present lower amounts of OPN protein. However, at later stages (21 days), cells are more aggregated and secreted more human OPN, creating a peripheral continuous layer. Furthermore, CLSM images also show that on Coll/nanoHA_Fb and Coll/nanoHA 3D biocomposite scaffolds, at 7 and 21 days of culture, the human OPN protein is well distributed and seemed to follow the irregularities of the materials' surfaces in accordance with the higher number of cells. In contrary, on both scaffolds, on 14th day it shows a decrease in OPN presence and cells.

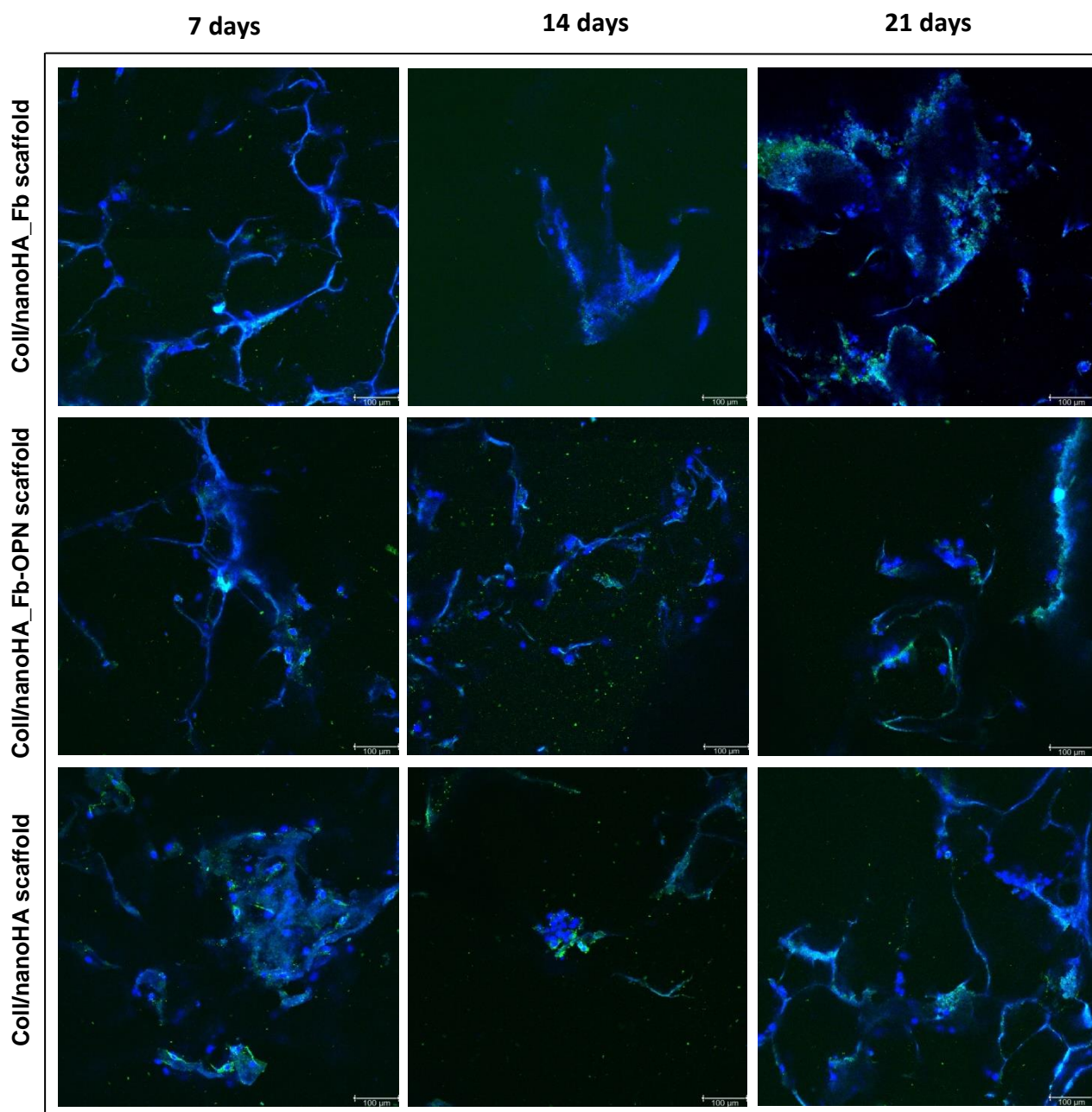


Figure 17- CLSM images showed the human osteogenic ECM (OPN) regarding hDFMSCs after 7, 14 and 21 days of culture within Coll/nanoHA_Fb scaffold (with and without OPN) and Coll/nanoHA scaffold. hDFMSCs nuclei were stain in blue and human OPN in green. Scale bar: 100 μm.

hDFMSCs morphology and distribution within Coll/nanoHA_Fb, Coll/nanoHA_Fb-OPN and Coll/nanoHA biocomposite scaffolds after 7, 14 and 21 days of culture were observed using CLSM. The pore walls of all samples are covered by the cell monolayer, which seems to follow the irregularities of the materials' surface, as illustrated in Figure 18. CLSM images also show that hDFMSCs seeded on Coll/nanoHA_Fb-OPN biocomposite scaffold were well spread entirely covering the scaffolds surfaces. In addition, at a later time-point of culture, it is possible to observe the highest number of cells creating

continuous cell layer over the material's surface. Thus, at 21st day of culture, the Coll/nanoHA_Fb-OPN scaffold shows the highest cell density (cellular aggregates). On the contrary, Coll/nanoHA_Fb and Coll/nanoHA scaffolds had a lower number of cells and present a more wide-spread distribution. Moreover, it is well observed that at early time-points cells display a spread and well adhered morphology, essentially within Coll/nanoHA_Fb and Coll/nanoHA scaffolds and at the latest time-points of culture hDFMSCs became rounder and agglomerated, mainly within the 3D biocomposite modified with OPN.

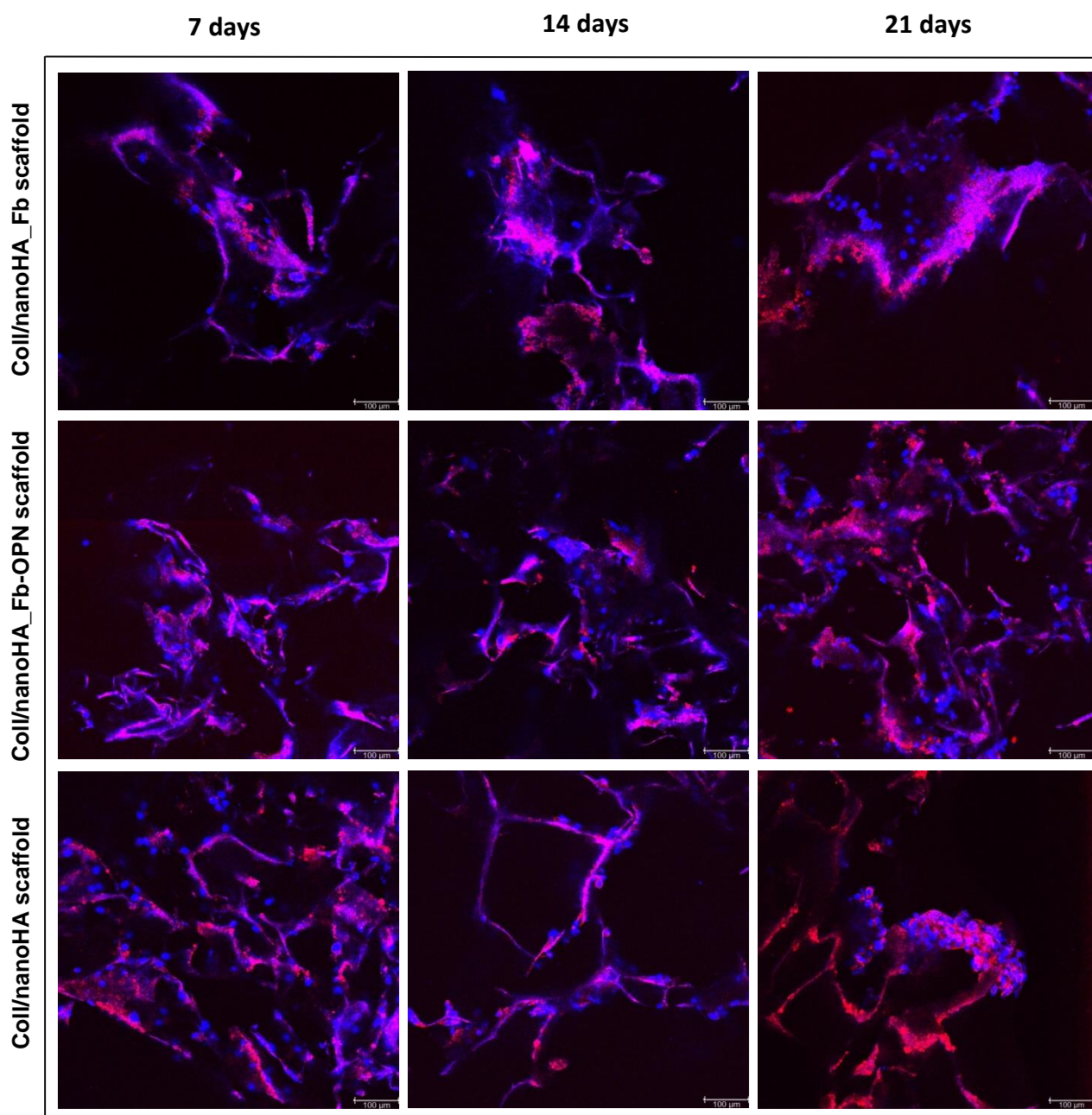


Figure 18- CLSM images showed the morphology of hDFMSCs after 7, 14 and 21 days of culture within a Coll/nanoHA_Fb scaffold (with and without OPN) and Coll/nanoHA scaffold. hDFMSCs nuclei were stain in blue and cytoplasm (actin filaments) in red. Scale bar: 100 μm.

CHAPTER 5

Discussion

Chapter 5- Discussion

The main goal of this master thesis work was to develop a biomimetic 3D Coll/nanoHA porous scaffold containing tooth-derived stem cells (from dental follicle tissue) loaded in a Fb-OPN hydrogel in order to fully regenerate bone tissue and improve early recovery of patients with critical maxillofacial bone defects. The application of hDFMSC in 3D biomimetic scaffolds with the purpose of bone tissue engineering has not been totally explored yet. Overall, this study explored the use of hDFMSC as a clinical alternative source for bone tissue engineering together with an innovative 3D Coll/nanoHA_Fb-OPN porous biomimetic scaffold.

Human osteoblast-like cell line (MG63) obtained from human osteosarcoma was first used in this work as a pilot study with bone cell lines to validate the protocol of cell delivery since it is a quite reproducible cell line. It also contributes to our understanding of osteoblast function, being well-characterized and a good model for examining the early stages of osteoblast differentiation and to test the materials' biocompatibility. Studies have shown numerous osteoblastic differentiations within biomaterials that are typical of bone-forming cells, including synthesis of collagen types I and III, the stimulation of alkaline phosphatase activity, osteocalcin synthesis and inhibition of proliferation in response to treatment with calcitriol (1,25-dihydroxyvitamin D3). Thus, as confirmed in this study, these cells exhibit a fast cell growth rate with doubling times of 3–4 days when compared to mature osteoblasts and so, have been used as an experimental model to study bone cell viability, adhesion, ECM synthesis, alkaline phosphatase activity, and osteocalcin production [64,65].

Previous assays were performed to evaluate the advantage of the incorporation of a fibrin hydrogel into a Coll/nanoHA scaffold (Appendix A) and also to study the differences in the cellular proliferation (DNA content) between Coll/nanoHA and Coll/nanoHA_Fb biocomposite scaffolds cultured with a basic medium or an osteoinductive cell culture medium (Appendix B). The osteogenic differentiation cocktail used was the combination of dexametasone and β -glycerophosphate. The later provided a phosphate donor that is required to build up the mineral phase. For instance, dexamethasone, a synthetic steroid, has been reported to enhance MG63 osteogenic differentiation [66]. Nevertheless, MG63 cultured within Coll/nanoHA_Fb scaffolds with basic medium showed higher proliferation capacity.

A studied biomimetic approach to improve cell attachment has been the modification of biomaterials with an arginine-glycine-aspartic-acid (RGD) motif [67]. OPN protein contains this sequence, being capable of binding cells by their surface receptors, promoting the cellular attachment to materials' substrate and their differentiation. OPN has also been considered a key factor in the recruitment of osteoblasts all along the initial stages of bone formation [67]. Therefore, these OPN enhanced the cell-surface interaction and promote high cell proliferation, differentiation and matrix synthesis, undoubtedly facilitating bone

regeneration [68]. Furthermore, OPN has been proposed to regulate many other physiological processes such as collagen organization, cell adhesion, cell viability, cell migration, angiogenesis and calcification since it has several binding sites with HA crystals, collagen and calcium ions [67,69].

The DNA quantification assay is a simple and accurate *in vitro* test that quantifies the proliferation rate of live cells. The higher the DNA content, the higher the cell mitosis activity and, subsequently, the number of cells. MG63 osteoblast-like cell proliferation within Coll/nanoHA and Coll/nanoHA_Fb scaffold with and without OPN was evaluated. As confirmed by the literature, Coll/nanoHA scaffold resulted in an overall inferior cellular proliferation rate due to its low mechanical strength, which does not provide the optimal environment for cell to growth and proliferate [70]. A previous *in vitro* biological study performed by Tsai *et al.* [71], showed that nanoHA aggregates have a key role in enhancing the osteoblastic phenotype expression level leading to an improved functional activity of the bone-derived cells. It is well known that the presence of the nanoHA aggregates induce a rougher surface topography which favours cell adhesion and proliferation. However, it is the incorporation of a dense Fb structure that provides a compact environment for cells to proliferate and stay viable, which is confirmed by the higher DNA content showed in Coll/nanoHA_Fb scaffold with and without OPN [72,73]. It was expected that the number of cells would increase in the presence of OPN once this protein favours cell adhesion. Nevertheless, higher proliferation rate was observed in the Coll/nanoHA_Fb scaffold although an increase in the total DNA content was also showed in the Coll/nanoHA_Fb-OPN scaffold (Fig. 8).

Alkaline phosphatase activity (ALP) *in vitro* assay is a quantitative analysis of this enzyme that is a commonly used parameter to evaluate the expression of the osteoblastic phenotype at an earlier stage of cell differentiation [62]. As described by Stein *et al.* [74], and Rowe *et al.* [75], the ALP activity increases during synthesis and maturation of the extracellular matrix, which matches to the beginning of cell differentiation to bone cells phenotype. The results of ALP activity for the MG63 culture showed that biocomposite scaffolds modified with OPN protein, in comparison with scaffolds without OPN, presented higher cellular differentiation capacity, although differences were not statistically expressive. However, a lower activity of ALP was detected with the MG63 within the Coll/nanoHA_Fb-OPN scaffolds ranging from 3rd to 14th day. Those results are in accordance with those from Dong *et al.* [76], Liu *et al.* [77], and Noda *et al.* [78] that reported an increase in ALP activity until the cell culture reaches higher cellular confluence, decreasing then its activity. In this case, cells possibly reached confluence at day 14 of culture, which led to the decrease in ALP levels after that time (Fig. 10).

The total protein content showed the amount of protein secreted by MG63 cells and presented in the ECM. Consequently, the higher ECM proteins concentration the higher the cells' viability and proliferation. As MG63 cells are in the beginning of the differentiation stage of the osteogenic genotype (pre-osteoblasts), they produce substantial quantity of proteins and a previous work published by Wang *et al.* [79], showed that at the last state of differentiation, cells were able to produce more ECM proteins for the matrix mineralization.

The results achieved with this work showed an increase in the overall amount of protein content in the ECM of Coll/nanoHA_Fb-OPN composite scaffold that reaches its concentration peak in the later stages of cell culture (Fig. 9). Previous work done by Salgado *et al.* [5], showed that modified cryogels Coll/nanoHA scaffolds were able to promote cell adhesion, proliferation and differentiation into osteoblastic phenotype. Other works done by Rodrigues *et al.* [63] and Yoshida *et al.* [61], showed that the Coll/nanoHA biocomposite had higher cell migration and proliferation when compared to the Collagen scaffolds. CLSM images corroborate these results with Coll/nanoHA_Fb-OPN biocomposite scaffolds presenting the highest cell viability and density, promoting an organized new bone extracellular matrix (human OPN) formation capable of covering all the material structure and thus, showing their capacity to differentiate *in vitro* within the scaffold (Fig. 11 and Fig.13).

Stem cells have been isolated from a variety of tissues, such as bone marrow, periosteum, muscle, adipose tissue and skin, however, for stem cell isolation it is usually necessary an invasive surgical procedure. Also, bone marrow-derived MSCs present significant age-related decrease in differentiation potential and frequency [80]. To overcome these limitations, human dental mesenchymal cells, in particular hDFMSC, have raised interest in the field of regenerative medicine since they can be isolated from extracted impacted third molars which are usually discarded as a dental medical waste, with no requiring needed of an extra surgery [81]. Furthermore, this neural crest originated cells, display other superiorities such as the easy accessibility, high viability and proliferation rate, active self-renewal capability, immunomodulatory properties, feasible cryopreservation and absence of ethical related issues [80,82-84].

To clarify the cellular basis of tissue regeneration, evaluating the multipotential capabilities of stem cells to differentiate into the desired target tissue is vitally important [85]. hDFMSCs contain a multipotent capacity of differentiation with high pluripotency and plasticity, as they can differentiate into osteoblasts, chondrocytes, adipocytes, cardiomyocytes, hepatocytes, neuronal cells, fibroblasts, cementoblasts, salivary gland cells, ductal cells and periodontal ligament cells [82,84]. In accordance with Rezai-Rad *et al.*, [81], DFSCs have strong osteogenic capability to differentiate toward the osteoblastic lineage. Graziano *et al.* [85], confirmed that dental mesenchymal cells are a promising source for bone tissue regeneration regarding their high capacity to adhere to biomaterials' surface.

Scaffold composition and surface properties are key factors in achieving bone tissue regeneration with an adequate osteogenic differentiation of dental mesenchymal cells [60]. In comparison with simple polymeric materials, composite biomaterials reinforced with calcium phosphate ceramics exhibited higher mechanical stability allied to lower degradation. This type of scaffolds has also shown to possess osteoconductive properties to MSCs with the expression of osteoblast-like gene markers [86]. Rodrigues *et al.* [63], and Salgado *et al.* [5,87], studies showed that with the integration of nanoHA in scaffolds it was possible to recruit bone marrow MSCs and boost their osteogenic differentiation.

Although there have been applications of dental stem cells in tissue regeneration, a reduced number of studies have introduced hDFMSCs to 3D tissue regeneration. Salgado and collaborators [80], cultured hDFMSCs in 3D porous scaffolds of collagen-nanohydroxyapatite with phosphoserine (collagen-nano-HA/OPS), an osteogenic inductor. These 3D hDFMSCs-loaded collagen-nano-HA/OPS scaffolds showed higher secreted levels of OPN with greater osteogenic differentiation.

Carvalho *et al.* [67], studied biomimetic OPN-enhanced collagen matrices presenting enhanced cell proliferation, promoting early MSCs osteogenic differentiation and angiogenesis, and showing a sustained bone formation response resulting in mineralized tissue similar to bone. The results of this work also showed the ability of hDFMSCs, cultured within Coll/nanoHA_Fb-OPN biocomposite scaffolds to proliferate and differentiate into osteoblastic cells, with higher DNA content and ALP enzyme activities. DNA extraction quantification showed a higher overall cell proliferation rate in Coll/nanoHA_Fb-OPN biomimetic scaffold (Fig. 14). Functional activity tests of hDFMSCs also presented favourable results in the OPN modified scaffold, showing gradual increase of ALP activity from early stages of differentiation (7 days) to later osteogenic maturation stages (21 days – Fig. 16). Moreover, in accordance with previous works performed by Salgado *et al.* [80], Schwartz *et al.* [88], and Carvalho *et al.* [64], all the materials that presented reduced rates of proliferation also showed expanding rates of its osteogenic differentiation capacity, due to a rise in the ALP activity. This behavior was a clear result that should end-up by leading to tissue growth for application for clinical purpose.

The results of the assessment of total protein content showed a global protein increase rate in Coll/nanoHA_Fb-OPN scaffolds in comparison to other samples (Fig. 15). This means that hDFMSCs are secreting more ECM proteins for the matrix mineralization in the 3D scaffold with OPN modification. CLSM images confirmed the highest hDFMSCs density within Coll/nanoHA_Fb-OPN scaffolds. Cellular aggregates with a round shape formed a continuous cell layer over the material's surface with major OPN secretion and thus, showing their capacity to differentiate *in vitro* within the OPN-modified scaffold (Fig. 17 and Fig.18). Mori *et al.* [83], showed that hDFMSCs cultured in favorable conditions show increased ALP activity, and formed *in vitro* mineralized matrix nodules.

CHAPTER 6

Conclusion and Future Outlook

Chapter 6- Conclusion and Future Outlook

Bone fractures and osteo-degenerative diseases prompt bone defects and, therefore, there is an increasing demand worldwide of fracture repair and bone regeneration solutions. With that purpose, the development of new techniques that accelerate fracture healing process, enhance bone regeneration and remodeling and result in new bone tissue that is similar to natural tissue structure and function is an urgent need. The main challenge is to successfully promote the materials' integration and bone tissue regeneration. Those bone regenerative needs foster the development of an injectable cell-loaded hydrogel with high bioactivity and a 3D scaffold with appropriate mechanical support to allow biocompatibility, biodegradability, stability to induce angiogenesis as well as achieving an optimal transport of nutrients, oxygen and growth factors. To address this challenge, this master thesis project developed a biomimetic Coll/nanoHA_Fb-OPN scaffold that delivers patient's cells and promotes the materials engraftment into the host tissue, providing a novel solution with considerable advantages over the current therapies, thus reducing patients' residence in hospital and surgery time, preventing post-surgery complications while improving patients' quality of life with a more cost-effective healthcare.

Coll/nanoHA 3D porous scaffold may enhance bone regeneration by creating and maintaining the biological space that supports progenitor cell attachment, migration, proliferation, differentiation and ECM deposition. Fibrin gel possesses a network structure, injectability and stability. OPN has a vital role in the recruitment of bone cells during the early stage of bone regeneration, enhancing cell proliferation and promoting early dental MSCs osteogenic differentiation. In conclusion, it was proved that Coll/nanoHA_Fb biocomposite with the presence of OPN protein promoted an increase in the materials' osteoinduction. The 3D construct promoted higher biocompatibility and dental MSC differentiation, with a higher capacity in promoting new ECM formation providing characteristics similar to the normal bone tissue and favoring its application in bone tissue engineering. In a future work, Coll/nanoHA_Fb-OPN with hDFMSCs may be tested in pre-clinical animal models as a proof of concept for their potential to promote the reconstruction of large and irregular bone defects for personalized needs.

References

- [1] Pedrero SG, Llamas-Sillero P, Serrano-López J. A Multidisciplinary Journey towards Bone Tissue Engineering. *Materials*. 2021;14(17):4896.
- [2] Nguyen LH, Annabi N, Nikkhah M, Bae H, Binan L, Park S, Kang Y, Yang Y, Khademhosseini A. Vascularized Bone Tissue Engineering: Approaches for Potential Improvement. *Tissue Eng. Part. B: Rev.* 2012;18(5):363-82.
- [3] O'Keefe RJ, Mao J. Bone tissue engineering and regeneration: from discovery to the clinic—an overview. *Tissue Eng Part B Rev.* 2011;17(6):389-92.
- [4] Amini AR, Laurencin CT, Nukavarapu SP. Bone tissue engineering: recent advances and challenges. *Crit Rev Biomed Eng.* 2012;40(5):363-408.
- [5] Salgado CL, Teixeira BIB, Monteiro FJM. Biomimetic Composite Scaffold With Phosphoserine Signaling for Bone Tissue Engineering Application. *Front Bioeng Biotechnol.* 2019;7:206.
- [6] Lorusso F, Inchingolo F, Dipalma G, Postiglione F, Fulle S, Scarano A. Synthetic Scaffold/Dental Pulp Stem Cell (DPSC) Tissue Engineering Constructs for Bone Defect Treatment: An Animal Studies Literature Review. *Int J Mol Sci.* 2020;21(24).
- [7] Ansari M. Bone tissue regeneration: biology, strategies and interface studies. *Prog Biomater.* 2019;8(4):223-37.
- [8] Brown JL, Laurencin CT. 2.6.6 - Bone Tissue Engineering. In: Wagner WR, Sakiyama-Elbert SE, Zhang G, Yaszemski MJ, editors. *Biomaterials Science (Fourth Edition)*: Academic Press; 2020. p. 1373-88.
- [9] Zhu L, Luo D, Liu Y. Effect of the nano/microscale structure of biomaterial scaffolds on bone regeneration. *Int J Oral Sci.* 2020;12(1):6.
- [10] Marks SC, Odgren PR. Chapter 1 - Structure and Development of the Skeleton. In: Bilezikian JP, Raisz LG, Rodan GA, editors. *Principles of Bone Biology (Second Edition)*. San Diego: Academic Press; 2002. p. 3-8.
- [11] Mateus AYP. Development, Characterisation and Application of Calcium Phosphates Nanocrystals Aggregates in a Collagen Matrix to be used as Biomaterial in Bone Regeneration [master's thesis on the Internet]. Porto (Portugal): University of Porto, Faculty of Engineering; 2010 [cited 2021 Nov 5]. Available from: <https://hdl.handle.net/10216/59713>
- [12] Brundavanam RK. Sonochemical synthesis, characterisation and biological evaluation of nano hydroxyapatite for potential hard tissue engineering applications [PhD's thesis on the Internet]. Australia: Murdoch University; 2013 [cited 2021 Nov 6]. Available from: <http://researchrepository.murdoch.edu.au/id/eprint/29172>

References

- [13] Yang Y. Skeletal morphogenesis during embryonic development. *Crit Rev Eukaryot Gene Expr.* 2009;19(3):197-218.
- [14] Shapiro F. Bone development and its relation to fracture repair. The role of mesenchymal osteoblasts and surface osteoblasts. *Eur Cell Mater.* 2008;15:53-76.
- [15] Armiento A, Hatt L, Sanchez Rosenberg G, Thompson K, Stoddart M. Functional Biomaterials for Bone Regeneration: A Lesson in Complex Biology. *Advanced Functional Materials.* 2020;30:1909874.
- [16] Hartmann C, Yang Y. Chapter 1 - Molecular and cellular regulation of intramembranous and endochondral bone formation during embryogenesis. In: Bilezikian JP, Martin TJ, Clemens TL, Rosen CJ, editors. *Principles of Bone Biology (Fourth Edition)*: Academic Press; 2020. p. 5-9.
- [17] Karaplis AC. Chapter 3 - Embryonic Development of Bone and the Molecular Regulation of Intramembranous and Endochondral Bone Formation. In: Bilezikian JP, Raisz LG, Rodan GA, editors. *Principles of Bone Biology (Second Edition)*. San Diego: Academic Press; 2002. p. 42-53.
- [18] Smith S, Varela A, Samadfam R. *Bone Toxicology*: Springer International Publishing; 2017.
- [19] Post TM, Cremers SC, Kerbusch T, Danhof M. Bone physiology, disease and treatment: towards disease system analysis in osteoporosis. *Clin Pharmacokinet.* 2010;49(2):89-118.
- [20] Lopes D, Martins-Cruz C, Oliveira MB, Mano JF. Bone physiology as inspiration for tissue regenerative therapies. *Biomaterials.* 2018;185:240-75.
- [21] Wang X, Xu S, Zhou S, Xu W, Leary M, Choong P, Qian M, Brandt M, Xie Y. Topological design and additive manufacturing of porous metals for bone scaffolds and orthopaedic implants: A review. *Biomaterials.* 2016;83:127-41.
- [22] Castillo Dalí G, Torres Lagares D. Chapter 1 - Nanobiomaterials in hard tissue engineering. In: Grumezescu AM, editor. *Nanobiomaterials in Hard Tissue Engineering*: William Andrew Publishing; 2016. p. 1-31.
- [23] Florencio-Silva R, Sasso GR, Sasso-Cerri E, Simões MJ, Cerri PS. Biology of Bone Tissue: Structure, Function, and Factors That Influence Bone Cells. *Biomed Res Int.* 2015;2015:421746.
- [24] Rossert J, Crombrughe B. Chapter 12 - Type I Collagen: Structure, Synthesis, and Regulation. In: Bilezikian JP, Raisz LG, Rodan GA, editors. *Principles of Bone Biology (Second Edition)*. San Diego: Academic Press; 2002. p. 189-XVIII.
- [25] Gelse K, Pöschl E, Aigner T. Collagens—structure, function, and biosynthesis. *Advanced Drug Delivery Reviews.* 2003;55(12):1531-46.

References

- [26] Garnero P. The Role of Collagen Organization on the Properties of Bone. *Calcified Tissue International*. 2015;97(3):229-40.
- [27] Patino MG, Neiders ME, Andreana S, Noble B, Cohen RE. Collagen: An Overview. *Implant Dentistry*. 2002;11(3):280-5.
- [28] Sheikh I, Dahman Y. Chapter 2 - Applications of nanobiomaterials in hard tissue engineering. In: Grumezescu AM, editor. *Nanobiomaterials in Hard Tissue Engineering*: William Andrew Publishing; 2016. p. 33-62.
- [29] Fung Y-C. Bone and Cartilage. In: Fung Y-C, editor. *Biomechanics: Mechanical Properties of Living Tissues*. New York, NY: Springer New York; 1993. p. 500-44.
- [30] Fröhlich M, Grayson WL, Wan LQ, Marolt D, Drobic M, Vunjak-Novakovic G. Tissue engineered bone grafts: biological requirements, tissue culture and clinical relevance. *Curr Stem Cell Res Ther*. 2008;3(4):254-64.
- [31] Lienemann PS, Lutolf MP, Ehrbar M. Biomimetic hydrogels for controlled biomolecule delivery to augment bone regeneration. *Adv Drug Deliv Rev*. 2012;64(12):1078-89.
- [32] Noda M, Denhardt DT. Chapter 15 - Osteopontin. In: Bilezikian JP, Raisz LG, Rodan GA, editors. *Principles of Bone Biology (Second Edition)*. San Diego: Academic Press; 2002. p. 239-48.
- [33] Gorski JP, Hankenson KD. Chapter 15 - Secreted noncollagenous proteins of bone. In: Bilezikian JP, Martin TJ, Clemens TL, Rosen CJ, editors. *Principles of Bone Biology (Fourth Edition)*: Academic Press; 2020. p. 368.
- [34] Hunter GK, Kyle CL, Goldberg HA. Modulation of crystal formation by bone phosphoproteins: structural specificity of the osteopontin-mediated inhibition of hydroxyapatite formation. *Biochem J*. 1994;300 (Pt 3):723-8.
- [35] Robey PG. Chapter 14 - Bone Matrix Proteoglycans and Glycoproteins. In: Bilezikian JP, Raisz LG, Rodan GA, editors. *Principles of Bone Biology (Second Edition)*. San Diego: Academic Press; 2002. p. 231.
- [36] Qu H, Fu H, Han Z, Sun Y. Biomaterials for bone tissue engineering scaffolds: a review. *RSC Advances*. 2019;9(45):26252-62.
- [37] Simorgh S, Milan PB, Saadatmand M, Bagher Z, Gholipourmalekabadi M, Alizadeh R, Hivechi A, Arabpour Z, Hamidi M, Delattre C. Human Olfactory Mucosa Stem Cells Delivery Using a Collagen Hydrogel: As a Potential Candidate for Bone Tissue Engineering. *Materials*. 2021;14(14):3909.
- [38] Oryan A, Alidadi S, Moshiri A, Maffulli N. Bone regenerative medicine: classic options, novel strategies, and future directions. *J Orthop Surg Res*. 2014;9(1):18.

References

- [39] Akter F, Ibanez J. Chapter 8 - Bone and Cartilage Tissue Engineering. In: Akter F, editor. *Tissue Engineering Made Easy*: Academic Press; 2016. p. 77-97.
- [40] Dimitriou R, Jones E, McGonagle D, Giannoudis PV. Bone regeneration: current concepts and future directions. *BMC Med*. 2011;9:66.
- [41] RF Canadas, S Pina, AP Marques, JM Oliveira, RL Reis. Chapter 7 - Cartilage and Bone Regeneration—How Close Are We to Bedside? In: *Translating Regenerative Medicine to the Clinic*, J. Laurence, Ed. Boston: Academic Press, 2016, pp. 89-106.
- [42] O'Brien FJ. Biomaterials & scaffolds for tissue engineering. *Materials Today*. 2011;14(3):88-95.
- [43] Filippi M, Born G, Chaaban M, Scherberich A. Natural Polymeric Scaffolds in Bone Regeneration. *Front Bioeng Biotechnol*. 2020;8:474.
- [44] Yue S, He H, Li B, Hou T. Hydrogel as a Biomaterial for Bone Tissue Engineering: A Review. *Nanomaterials (Basel)*. 2020;10(8).
- [45] Zhang Y, Li Z, Guan J, Mao Y, Zhou P. Hydrogel: A potential therapeutic material for bone tissue engineering. *AIP Advances*. 2021;11(1):010701.
- [46] Lee H, Yoo JM, Nam SY. Additive Fabrication and Characterization of Biomimetic Composite Bone Scaffolds with High Hydroxyapatite Content. *Gels*. 2021;7(3):100.
- [47] Bai X, Gao M, Syed S, Zhuang J, Xu X, Zhang X-Q. Bioactive hydrogels for bone regeneration. *Bioact Mater*. 2018;3(4):401-17.
- [48] Ullah F, Othman MB, Javed F, Ahmad Z, Md Akil H. Classification, processing and application of hydrogels: A review. *Mater Sci Eng C Mater Biol Appl*. 2015;57:414-33.
- [49] Zhao W, Jin X, Cong Y, Liu Y, Fu J. Degradable natural polymer hydrogels for articular cartilage tissue engineering. *Journal of Chemical Technology and Biotechnology*. 2013;88.
- [50] Sordi MB, Cruz A, Fredel MC, Magini R, Sharpe PT. Three-dimensional bioactive hydrogel-based scaffolds for bone regeneration in implant dentistry. *Mater Sci Eng C Mater Biol Appl*. 2021;124:112055.
- [51] Liu M, Zeng X, Ma C, Yi H, Ali Z, Mou X, et al. Injectable hydrogels for cartilage and bone tissue engineering. *Bone Res*. 2017;5:17014.
- [52] Sun Y, Nan D, Jin H, Qu X. Recent advances of injectable hydrogels for drug delivery and tissue engineering applications. *Polymer Testing*. 2019;81:106283.
- [53] Noori A, Ashrafi SJ, Vaez-Ghaemi R, Hatamian-Zaremi A, Webster TJ. A review of fibrin and fibrin composites for bone tissue engineering. *Int J Nanomedicine*. 2017;12:4937-61.

References

- [54] Sproul E, Nandi S, Brown A. Chapter 6 - Fibrin biomaterials for tissue regeneration and repair. In: Peptides and Proteins as Biomaterials for Tissue Regeneration and Repair, M. A. Barbosa and M. C. L. Martins, Eds.: Woodhead Publishing, 2018, pp. 151-173.
- [55] Linsley CS, Wu BM, Tawil B. Mesenchymal stem cell growth on and mechanical properties of fibrin-based biomimetic bone scaffolds. *Journal of Biomedical Materials Research Part A*. 2016;104(12):2945-53.
- [56] Janmey PA, Winer JP, Weisel JW. Fibrin gels and their clinical and bioengineering applications. *J R Soc Interface*. 2009;6(30):1-10.
- [57] Matichescu A, Ardelean LC, Rusu LC, Craciun D, Bratu EA, Babucea M, Leretter M. Advanced Biomaterials and Techniques for Oral Tissue Engineering and Regeneration-A Review. *Materials (Basel)*. 2020;13(22).
- [58] Funda G, Taschieri S, Bruno GA, Grecchi E, Paolo S, Girolamo D, Fabbro M. Nanotechnology Scaffolds for Alveolar Bone Regeneration. *Materials (Basel)*. 2020;13(1).
- [59] Shang F, Yu Y, Liu S, Ming L, Zhang Y, Zhou Z, Zhao J, Jin Y. Advancing application of mesenchymal stem cell-based bone tissue regeneration. *Bioact Mater*. 2021;6(3):666-83.
- [60] Granz CL, Gorji A. Dental stem cells: The role of biomaterials and scaffolds in developing novel therapeutic strategies. *World J Stem Cells*. 2020;12(9):897-921.
- [61] Yoshida T, Kikuchi M, Koyama Y, Takakuda K. Osteogenic activity of MG63 cells on bone-like hydroxyapatite/collagen nanocomposite sponges. *J Mater Sci Mater Med*. 2010;21(4):1263-72.
- [62] Ren L, Tsuru K, Hayakawa S, Osaka A. Novel approach to fabricate porous gelatin-siloxane hybrids for bone tissue engineering. *Biomaterials*. 2002;23(24):4765-73.
- [63] Rodrigues SC, Salgado CL, Sahu A, Garcia MP, Fernandes MH, Monteiro FJ. Preparation and characterization of collagen-nanohydroxyapatite biocomposite scaffolds by cryogelation method for bone tissue engineering applications. *J Biomed Mater Res A*. 2013;101(4):1080-94.
- [64] Price N, Bendall SP, Frondoza C, Jinnah RH, Hungerford DS. Human osteoblast-like cells (MG63) proliferate on a bioactive glass surface. *J Biomed Mater Res*. 1997;37(3):394-400.
- [65] Clover J, Gowen M. Are MG-63 and HOS TE85 human osteosarcoma cell lines representative models of the osteoblastic phenotype? *Bone*. 1994;15(6):585-91.
- [66] Kadar K, Kiraly M, Porcsalmy B, Molnar B, Racz GZ, Blazsek J, Kallo K, Szabo EL, Gera Eu, Gerber G, Varga G. Differentiation potential of stem cells from human dental origin - promise for tissue engineering. *J Physiol Pharmacol*. 2009;60 Suppl 7:167-75.

References

- [67] Carvalho MS, Poundarik AA, Cabral JMS, da Silva CL, Vashishth D. Biomimetic matrices for rapidly forming mineralized bone tissue based on stem cell-mediated osteogenesis. *Sci Rep*. 2018;8(1):14388.
- [68] Chan WD, Perinpanayagam H, Goldberg HA, Hunter GK, Dixon SJ, Santos GC, Rizkalla AS. Tissue engineering scaffolds for the regeneration of craniofacial bone. *J Can Dent Assoc*. 2009;75(5):373-7.
- [69] Makishi S, Yamazaki T, Ohshima H. Osteopontin on the Dental Implant Surface Promotes Direct Osteogenesis in Osseointegration. *Int J Mol Sci*. 2022;23(3).
- [70] Parmar A, Ansari NA, Parmar G, Krishnakumar A. Evaluation of cell viability of Human Dental Pulp Stem Cells in Two dimensional and Three dimensional Fibrin Glue Scaffold. *J Conserv Dent*. 2020;23(5):479-83.
- [71] Tsai SW, Hsu FY, Chen PL. Beads of collagen-nanohydroxyapatite composites prepared by a biomimetic process and the effects of their surface texture on cellular behavior in MG63 osteoblast-like cells. *Acta Biomater*. 2008;4(5):1332-41.
- [72] Deligianni DD, Katsala ND, Koutsoukos PG, Missirlis YF. Effect of surface roughness of hydroxyapatite on human bone marrow cell adhesion, proliferation, differentiation and detachment strength. *Biomaterials*. 2001;22(1):87-96.
- [73] Brunette DM. The effects of implant surface topography on the behavior of cells. *Int J Oral Maxillofac Implants*. 1988;3(4):231-46.
- [74] Stein GS, Lian JB, Owen TA. Relationship of cell growth to the regulation of tissue-specific gene expression during osteoblast differentiation. *Faseb j*. 1990;4(13):3111-23.
- [75] Rowe SL, Lee S, Stegemann JP. Influence of thrombin concentration on the mechanical and morphological properties of cell-seeded fibrin hydrogels. *Acta Biomater*. 2007;3(1):59-67.
- [76] Dong SW, Ying DJ, Duan XJ, Xie Z, Yu ZJ, Zhu CH, et al. Bone regeneration using an acellular extracellular matrix and bone marrow mesenchymal stem cells expressing Cbfa1. *Biosci Biotechnol Biochem*. 2009;73(10):2226-33.
- [77] Liu H, Li W, Shi S, Habelitz S, Gao C, Denbesten P. MEPE is downregulated as dental pulp stem cells differentiate. *Arch Oral Biol*. 2005;50(11):923-8.
- [78] Noda M, Rodan GA. Type-beta transforming growth factor inhibits proliferation and expression of alkaline phosphatase in murine osteoblast-like cells. *Biochem Biophys Res Commun*. 1986;140(1):56-65.
- [79] Wang C, Meng H, Wang X, Zhao C, Peng J, Wang Y. Differentiation of Bone Marrow Mesenchymal Stem Cells in Osteoblasts and Adipocytes and its Role in Treatment of Osteoporosis. *Med Sci Monit*. 2016;22:226-33.

References

- [80] Salgado CL, Barrias CC, Monteiro FJM. Clarifying the Tooth-Derived Stem Cells Behavior in a 3D Biomimetic Scaffold for Bone Tissue Engineering Applications. *Front Bioeng Biotechnol.* 2020;8:724.
- [81] Rezai-Rad M, Bova JF, Orooji M, Pepping J, Qureshi A, Del Piero F, Hayes D, Yao S. Evaluation of bone regeneration potential of dental follicle stem cells for treatment of craniofacial defects. *Cytotherapy.* 2015;17(11):1572-8.
- [82] Bi R, Lyu P, Song Y, Li P, Song D, Cui C, Fan Y. Function of Dental Follicle Progenitor/Stem Cells and Their Potential in Regenerative Medicine: From Mechanisms to Applications. *Biomolecules.* 2021;11(7):997.
- [83] Mori G, Ballini A, Carbone C, Oranger A, Brunetti G, Di Benedetto A, Rapone B, Cantore S, Di Comite M, Colucci S, Grano M, Grassi F. Osteogenic differentiation of dental follicle stem cells. *Int J Med Sci.* 2012;9(6):480-7.
- [84] Zhang J, Ding H, Liu X, Sheng Y, Liu X, Jiang C. Dental Follicle Stem Cells: Tissue Engineering and Immunomodulation. *Stem Cells Dev.* 2019;28(15):986-94.
- [85] Graziano A, d'Aquino R, Laino G, Papaccio G. Dental pulp stem cells: a promising tool for bone regeneration. *Stem Cell Rev.* 2008;4(1):21-6.
- [86] McCafferty MM, Burke GA, Meenan BJ. Calcium phosphate thin films enhance the response of human mesenchymal stem cells to nanostructured titanium surfaces. *J Tissue Eng.* 2014;5:2041731414537513.
- [87] Salgado CL, Grenho L, Fernandes MH, Colaço BJ, Monteiro FJ. Biodegradation, biocompatibility, and osteoconduction evaluation of collagen-nanohydroxyapatite cryogels for bone tissue regeneration. *J Biomed Mater Res A.* 2016;104(1):57-70.
- [88] Schwartz Z, Lohmann CH, Oefinger J, Bonewald LF, Dean DD, Boyan BD. Implant surface characteristics modulate differentiation behavior of cells in the osteoblastic lineage. *Adv Dent Res.* 1999;13:38-48.

Appendix A

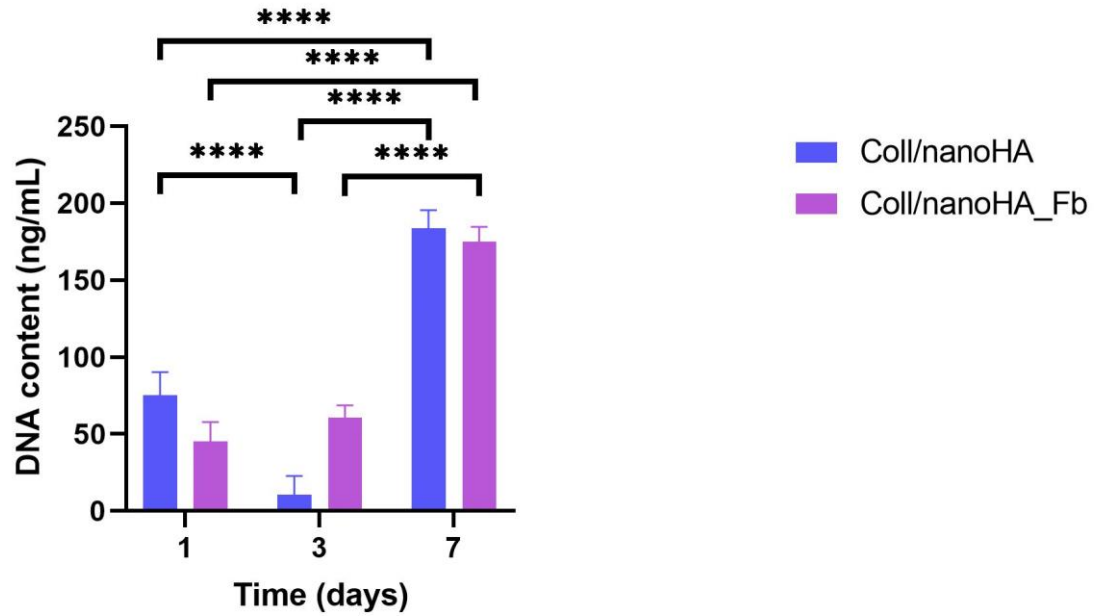


Figure 19- Total DNA content of MG63 osteoblast-like cells within Coll/nanoHA and Coll/nanoHA_Fb biocomposite scaffolds after 1, 3 and 7 days of culture in basic medium. Statistical differences between samples from different time-points (**** $p < 0.0001$).

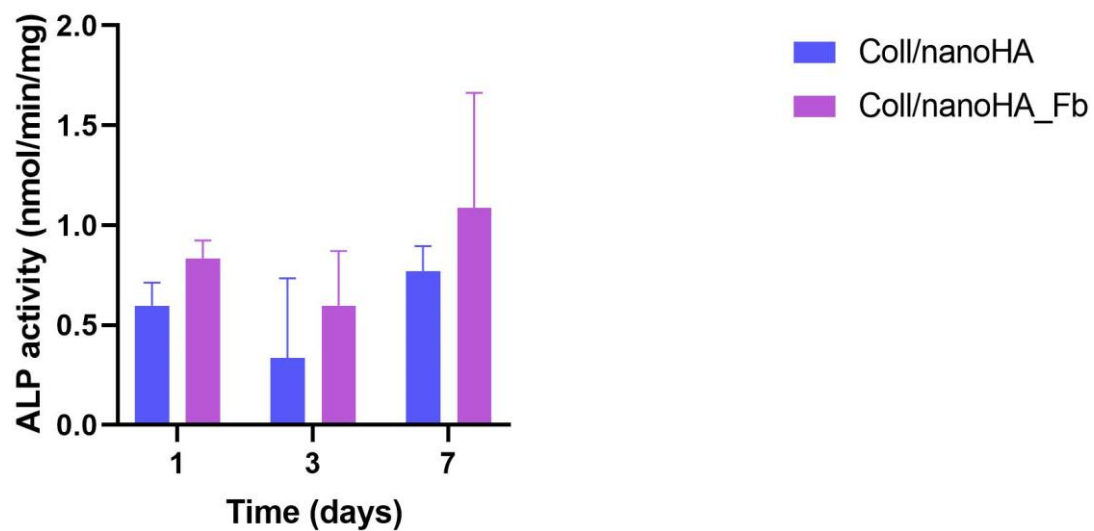


Figure 20- ALP activity of MG63 osteoblast-like cells within Coll/nanoHA and Coll/nanoHA_Fb biocomposite scaffolds after 1, 3 and 7 days of culture. Statistical differences ($p > 0.05$) were not observed.

Appendix B

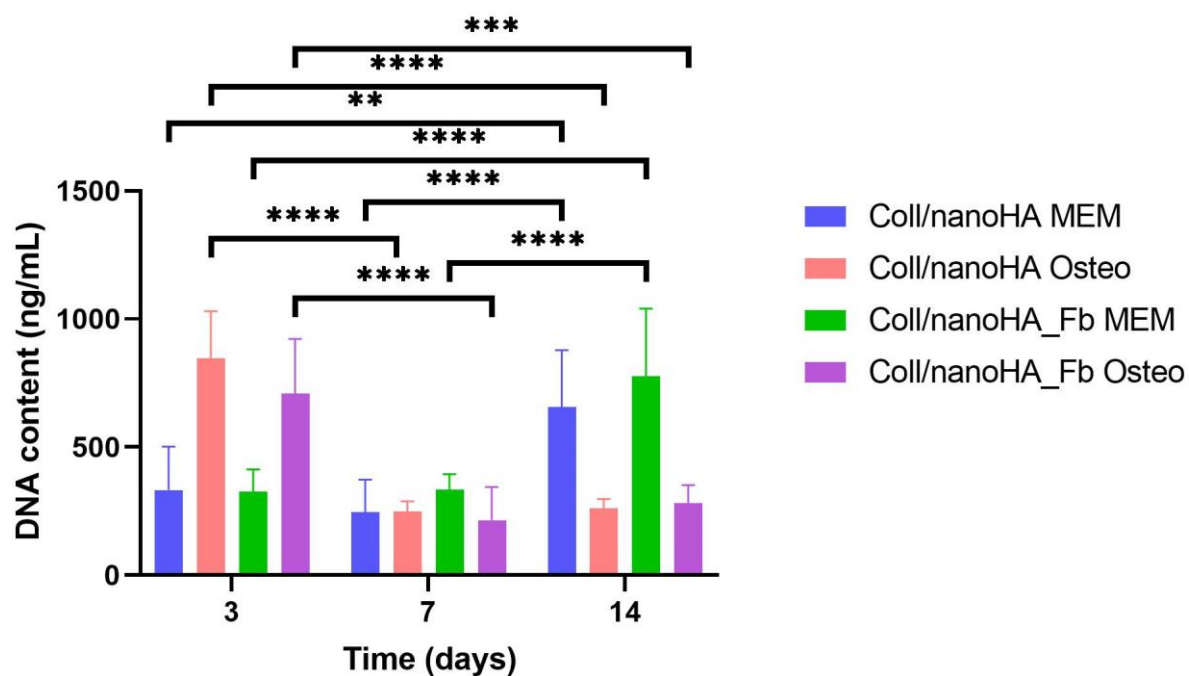


Figure 21- Total DNA content of MG63 osteoblast-like cells within Coll/nanoHA and Coll/nanoHA_Fb biocomposite scaffolds after 3, 7 and 14 days of culture in basic and osteoinductive medium. Statistical differences between samples from different time-points, **p < 0.01, ***p < 0.001 and ****p < 0.0001.



DECLARAÇÃO

Monografia/Relatório de Estágio

Declaro que o presente trabalho, no âmbito da Monografia/Relatório de Estágio, integrado no MIMD, da FMDUP, é da minha autoria e todas as fontes foram devidamente referenciadas.

Porto, 26 de maio de 2022

A Estudante,

Patrícia Nafalda Gonçalves Alves



PARECER DO ORIENTADOR

(Entrega do trabalho final de Monografia)

Informo que o Trabalho de Monografia/Relatório de Estágio desenvolvido pela estudante Patrícia Mafalda Gonçalves Alves com o título: "Development of dental MSC-loaded fibrin hydrogel injected into a 3D scaffold to drive bone tissue regeneration", está de acordo com as regras estipuladas na FMDUP, foi por mim conferido e encontra-se em condições de ser apresentado em provas públicas.

Porto, 26 de maio de 2022

A Orientadora,





PARECER DO COORIENTADOR

(Entrega do trabalho final de Monografia)

Informo que o Trabalho de Monografia/Relatório de Estágio desenvolvido pela estudante Patrícia Mafalda Gonçalves Alves com o título: "Development of dental MSC-loaded fibrin hydrogel injected into a 3D scaffold to drive bone tissue regeneration", está de acordo com as regras estipuladas na FMDUP, foi por mim conferido e encontra-se em condições de ser apresentado em provas públicas.

Porto, 26 de maio de 2022

O Coorientador,



DECLARAÇÃO
Mestrado Integrado em Medicina Dentária
Monografia/Relatório de Estágio

Identificação do autor

Nome completo Patrícia Nafalda Gonçalves Alves
N.º de identificação civil 15930335 N.º de estudante 201803494
Email institucional up201803494@fmd.up.pt
Email alternativo patriciamafaldaalves@gmail.com Tlf/Tlm 935421589
Faculdade/Instituto Faculdade de Medicina Dentária da Universidade do Porto

Identificação da publicação

Dissertação de Mestrado Integrado (Monografia) ☒

Relatório de Estágio ☐

Título completo

"Development of dental NSC-loaded fibrin hydrogel injected into
a 3D scaffold to drive bone tissue regeneration"

Orientador Christiane Laranjo Salgado

Coorientador Germano Neves Pinto da Rocha

Palavras-chave Biomaterials ; Hydrogel ; Fibrin ; Collagen ; Nanohydroxyapatite ;
Osteopontin ; Oral maxillofacial bone tissue regeneration

Autorizo a disponibilização imediata do texto integral no Repositório da U.Porto: _____ (x)

Não Autorizo a disponibilização imediata do texto integral no Repositório da U.Porto : _____ X (x)

Autorizo a disponibilização do texto integral no Repositório da U.Porto, com período de embargo, no prazo de:

6 Meses: _____ ; 12 Meses: _____ ; 18 Meses: _____ ; 24 Meses: X ; 36 Meses: _____ ; 120 Meses: _____ .

Justificação para a não autorização imediata Publicação de resultados

Data 26 / 05 / 2022

Assinatura Patrícia Nafalda Gonçalves Alves